DEVELOPMENT OF ANDROGEN RECEPTOR MESSENGER RNA TARGETED MOLECULAR BEACONS FOR USE IN THE STUDY OF PROSTATE CANCER PROGRESSION

A Thesis
Presented to
The Academic Faculty

By

Cindy Jennifer Glick

In Partial Fulfillment
Of the Requirements for the Degree
Master of Science in Bioengineering

Georgia Institute of Technology

December 2008

DEVELOPMENT OF ANDROGEN RECEPTOR MESSENGER RNA TARGETED
MOLECULAR BEACONS FOR USE IN THE STUDY OF PROSTATE CANCER
PROGRESSION

Approved by:

Dr. Gang Bao, Advisor
School of Biomedical Engineering
Georgia Institute of Technology

Dr. Philip Santangelo
School of Biomedical Engineering
Georgia Institute of Technology

Dr. Alfred Merrill
School of Biology
Georgia Institute of Technology

Date Approved: July 9, 2008

ACKNOWLEDGEMENTS

I would like to thank all of the members of the Laboratory of Biomolecular Engineering and Nanomedicine for their guidance, advice, and most of all for their friendship. Specifically, I would like to thank Charles Glaus, Dr. Won Jong Rhee, and Dr. Frances Lennon for their intellectual and moral support. I am also grateful for the help of Qingfen Pan, my undergraduate assistant. Without her work, my thesis would not be complete. I would also like to acknowledge Dr. Philip Santangelo, a former lab member, who helped me tremendously in more ways than I can count.

I would like to thank my family, especially my fiancé, Jeremy, for their encouragement and support throughout this entire process.

I would like to express my sincerest appreciation to Dr. Paul Rennie from the University of British Columbia for providing us with the hAR plasmid, Dr. Leland Chung from Emory University for his intellectual advisement, as well as my entire thesis committee for their part in this process.

It would also like acknowledge the sources of funding for this project: NIH Grants 1R01CA108468 and U54CA119338.

Finally, I would like to thank Dr. Gang Bao, the Principal Investigator of the Laboratory of Biomolecular Engineering and Nanomedicine, for giving me the opportunity to learn and grow in more ways than I thought I would.

TABLE OF CONTENTS

LIST OF TABLES

LIST OF FIGURES

NOMENCLATURE

AR = Androgen Receptor

mRNA = messenger RNA

AR+ = Androgen Receptor positive

AR- = Androgen Receptor negative

DHT = dihydrotestosterone

ARE = Androgen Response Element

CDK = Cyclin-dependent kinase

PSA = Prostate Specific Antigen

IL-6 = Interleukin-6

TNFα = tumor necrosis factor α

β-AR = β adrenergic receptor

CRD-BP = coding region determinant-binding protein

VEGF = vascular endothelial growth factor

AUF-1 = adenosine uridine-rich element/poly-(U) binding degradation factor 1

MAPK = mitogen-activated protein kinase

PKC = protein kinase C

PCBP = poly(C) RNA-binding protein

UTR = untranslated region

2'-O-Me = 2'-O-Methyl

GAPDH = glyceraldehyde 3-phosphate dehydrogenase

BMP-4 = bone morphogenetic protein 4

RSV = Respiratory Syncytial Virus

NCBI = National Center for Biotechnology Information

BLAST = Basic Local Alignment Search Tool

x

NaCl = sodium chloride

BHQ2 = Black Hole Quencher 2

dNTP = deoxyribonucleotide triphosphate

RT-PCR = reverse transcriptase polymerase chain reaction

SLO = Streptolysin O

TCEP = Tris(2-carboxyethyl)phosphine

siRNA = small interfering RNA

hAR plasmid = human Androgen Receptor plasmid

EtOH = ethanol

DMSO = dimethyl sulfoxide

NA = numerical aperture

FISH = Fluorescence in situ hybridization

ZBP2 = zipcode binding protein 2

eIF4G = eukaryotic translation initiation factor 4G

PABP = poly(A) binding protein

SUMMARY

Messenger RNA (mRNA) posttranscriptional regulation has been implicated in the development and/or progression of several diseases including many types of cancer, rheumatoid arthritis, vascular disease, and Alzheimer's disease. Differential regulation of Androgen Receptor (AR) mRNA has been associated specifically with prostate cancer progression.   In this thesis, molecular beacons were developed to allow for the detection of the expression and localization of AR mRNA in live prostate cancer cells. These beacons were then applied as a tool for studying how AR mRNA regulation is involved in prostate cancer growth and advancement. Two AR mRNA targeted beacons were designed and tested in solution and in live cells to determine their functionality. The beacon-based approach for AR mRNA detection was then optimized through the use of the two beacons in tandem and alteration of their backbone chemistry. A series of validation tests were performed on these beacons, including testing their abilities to: 1) produce a feasible localization pattern, 2) discriminate between AR positive (AR+) and AR negative (AR-) prostate cancer cell lines and 3) follow stimulus-induced changes in AR mRNA expression. Based on these results, a dual chimeric beacon approach was selected to determine the role of AR mRNA regulation in two systems that represent important stages in prostate cancer growth and progression: 1) hormone stimulation of androgen-dependent prostate cancer cells and 2) progression of androgen-dependent prostate cancer cells to the androgen-independent state. Our results suggest that changes in AR mRNA expression, organization, and localization may be indicative of molecular mechanisms involved in these critical transitions associated with prostate cancer progression. Taken together, this work provides a feasibility study for visualizing changes in AR mRNA state as a diagnostic measure for evaluating the aggressiveness

of the disease and demonstrates the possible utility of therapeutically targeting AR

mRNA regulation in order to prevent prostate cancer advancement.

CHAPTER 1: INTRODUCTION

Understanding the molecular pathogenesis of prostate cancer progression has become exceedingly important due to the limited treatment options available once the disease has progressed beyond the early-stage androgen-dependent phase to the advanced androgen-independent state. The research presented in this thesis is concerned with the potential role of Androgen Receptor (AR) mRNA posttranscriptional regulation in promoting prostate cancer progression. In order to understand why we are interested in investigating this specific disease progression mechanism, it is first necessary to understand the role of AR in prostate cancer, the potential for mRNA regulation to be a player in disease progression, and specifically how AR mRNA is regulated and how this regulation could conceivably push both early-stage disease and lead to the development of the androgen-independent disease state.   We used molecular beacon technology to track AR mRNA in live prostate cancer cells in order to help elucidate the importance of posttranscriptional regulation on the progression of this disease. Learning more about how AR mRNA is regulated in prostate cancer could point to potential therapeutic targets as well as diagnostic indicators of disease advancement.

1.1 The Role of Androgen Receptor in Prostate Cancer Progression

Prostate cancer is the second most common form of cancer and the second leading cause of cancer related death for men in the United States. Early-stage prostate cancer is classified as androgen-dependent. This means that the cancer requires the presence of androgens to bind to and activate Androgen Receptor (AR), an intracellular hormone receptor present in the prostate gland, in order to for the cells to grow and divide. These early-stage androgen-dependent tumors are either surgically removed or treated with radiation to destroy the cancer cells. Tumors that are not eliminated through these

1

methods are often treated with androgen ablation therapy. In the absence of androgens, these tumors will regress. However, this treatment is often unsuccessful in the long term due to the progression of the cancer to the more aggressive androgen-independent form. (1)

AR activity is crucial throughout the course of prostate cancer. AR is activated when dihydrotestosterone (DHT), the reduced form of testosterone, binds to the receptor, leading to receptor dimerization, translocation to the nucleus, and binding of the AR dimer to Androgen Response Element (ARE) sequences in the promoter regions of target genes, altering their expression. Target genes include cell proliferation genes such as Cyclin dependent kinases (CDKs), Cyclins, growth factors, cell survival genes that suppress apoptosis, Prostate Specific Antigen (PSA), and AR itself. Therefore, increased AR activity and subsequent regulation of these target genes leads to increased cell division and decreased apoptosis.   (1)

As stated earlier, early-stage prostate cancer is dependent on the presence of androgens, mainly DHT, to activate AR. When prostate cancer is in this androgen-dependent state, a common method of treatment is to block AR activity through androgen ablation, which can be achieved through surgical or chemical castration. Some androgen ablation therapy drugs are 5α-reductase inhibitors such as finasteride that work by blocking the conversion of testosterone to DHT. Other drugs such as cyproterone acetate, flutamide, and bicalutamide function as DHT competitors that block site accessibility on AR. (2,3)   However, after period of 1 to 2 years, some prostate cancer cells can become resistant to androgen ablation therapy. (4) This population of cells will continue to grow and divide despite the absence of androgens, transforming the cancer into the more aggressive and less treatable androgen-independent form.

There are several ways that prostate cancer can transition to androgen-independence. One method is to increase the sensitivity of the cells to androgen so that low levels will be enough to push the growth pathway. Prostate cancer cells can achieve hypersensitivity to low levels of androgen through AR gene amplification, which in turn leads to increased AR protein production. AR gene amplification is present in about one-fifth to one-third of these advanced tumors. If prostate cancer cells undergo mutations that increase 5α-reductase activity, this will lead to increased conversion of testosterone to the more active DHT form, which will help push the AR pathway despite low levels of androgen. Mutations that make AR more stable and/or translocate to the nucleus more easily will also allow for the receptor to have increased activity even when androgen levels are low. (1-6)

A second method by which prostate cancer cells can become androgen-independent is through mutations in the AR gene that lowers the specificity of the receptor's binding site. Decreased specificity of the binding site will allow other molecules besides DHT to bind to and activate the receptor. This becomes increasingly problematic is cases where the AR gene is mutated so that the receptor responds to androgen-antagonists such as flutamide the same way that the receptor responds to androgens. When this happens, androgen ablation therapy won't only stop being effective, but it will become a harmful factor in promoting prostate cancer growth. (1-6)

A third method that can lead to this transition is when mutations occur that allow AR to be activated in a non-ligand-dependent manner. AR can be mutated to make it constitutively active or mutations may occur that allow for the activation of AR through other ligand-independent methods such as phosphorylation. (1-6)

3

Androgen-independence can also be achieved by bypassing the AR pathway altogether through genetic changes that push other growth pathways such as the Bcl-2 pathway. This will allow prostate cancer cells to grow in spite of the fact that the dominant AR pathway is no longer being pushed. In the case of AR- prostate cancer, mechanisms like these must be employed to allow for cancer cell growth and survival. (1-6)

 While all of these potential mechanisms for pushing prostate cancer into the androgen-independent phase are important potential therapeutic targets, we are interested investigating the mechanism by which prostate cancer cells employ differential AR mRNA posttranscriptional regulation in order to circumvent the need for androgen stimulation. (7) The potential importance of this mechanism will be discussed further in section 1.3.   But in order to understand why it is feasible that AR mRNA regulation could be critical for prostate cancer progression, it is first important to review other cases where posttranscriptional regulation has been implicated as an important player in the development and/or progression of disease.

1.2 Posttranscriptional Regulation of mRNA in Disease

Posttranscriptional regulation of mRNA plays an important role in regulating gene expression. A key way that mRNA is regulated is through the interaction of various RNA-binding proteins with *cis*-elements within the untranslated regions of an mRNA. These RNA-binding proteins can affect mRNA localization, stability, and translational efficiency. Changes in mRNA regulation have been associated with many diseases including cancer, arthritis, and Alzheimer's disease. (8)

Changes in mRNA stability have been a common alteration seen in several diseases. Crucial transcription factors such as C-myc, cytokines, and growth factors such as

4

Interleukin-6 (IL-6) often have higher mRNA stability in cancer cells because increased production of these proteins will push the cells to grow and divide. Tumor necrosis factor α (TNFα) is often mutated to increase mRNA stability in chronic inflammatory arthritis because accumulation of this protein supports this development of the disease. (8,9) A decrease in β adrenergic receptor (β-AR) mRNA stability has been shown to accompany low levels of β-ARs seen in patients with hypertension and myocardial failure. (9)

Differential posttranscriptional regulation can be caused by both mutations in protein binding sites within an mRNA as well as changes in RNA-binding protein expression. Changes in RNA-binding protein expression have been specifically associated with cancer development. For example, amplification of a key RNA-binding protein, coding region determinant-binding protein (CRD-BP), which binds to and stabilizes C-myc mRNA, has been found in approximately one-third of breast cancers. HuR is an RNA-binding protein that has been shown to be upregulated in several tumor types, including cancer of the nervous system. HuR promotes the cytoplasmic localization, stabilization, and translational efficiency of several cancer promoting mRNAs such as vascular endothelial growth factor (VEGF) and TNFα. (8) Upregulation of VEGF is particularly critical to the angiogenic processes required for tumor metastasis. In the case of β-AR mRNA destabilization previously discussed, this critical change in mRNA stability has been associated with the upregulation of a destabilizing RNA-binding protein, adenosine uridine-rich element/poly-(U) binding degradation factor 1 (AUF-1). (9)

Mutations in the protein binding elements within various disease-relevant mRNA and disease-associated differential expression of critical RNA-binding proteins have both become targets for pharmacological intervention. (9,10) By targeting the mRNA as

5

opposed to the protein it produces, you afford yourself the opportunity to disrupt a disease-associated pathway where the protein is inaccessible or highly mutated. (10) Since no drugs have been identified so far that can specifically disrupt an RNA-binding protein-mRNA interaction, research has turned to interfering with the synthesis and/or functional capabilities of these RNA-binding proteins. Signaling cascades such as the mitogen-activated protein kinase (MAPK) and protein kinase C (PKC) pathways regulate the expression of various mRNA stabilizing and destabilizing proteins, making them an attractive therapeutic target. (9)

Given the importance of mRNA posttranscriptional regulation in the development and progression of several diseases, the ability to visualize and track these critical mRNAs in live cells has the potential to be incredibly useful for studying these important biological mechanisms. Molecular beacons, which will be discussed in further detail in section 1.4, are probes used for the detection of mRNA in live cells. This technology could be a useful tool for allowing researchers to study mRNA regulation within these disease models. (11-13)

1.3 Posttranscriptional Regulation of AR mRNA in Prostate Cancer

Some researchers believe that AR mRNA posttranscriptional modifications, specifically those modifications affecting mRNA stability, are essential in controlling AR protein production in prostate cancer. RNA-binding proteins such as HuR and poly(C) RNA-binding proteins (PCBPs) are known to bind to elements within the 3'-untranslated region (UTR) of AR mRNA and influence the regulation of this message. This regulation of AR mRNA is thought to play a critical role in allowing for more efficient production and distribution of AR protein within the cell, which can push prostate cancer growth without the dependence on androgen stimulation. (7,14,15)

6

AR mRNA posttranscriptional regulation also plays a role in androgen-dependent prostate cancer. While DHT or synthetic androgen stimulation increases AR protein levels in androgen-dependent prostate cancer, including the AR+ androgen-dependent LNCaP cell line, it illogically causes a decrease in the AR mRNA levels of these cells. (16-20) However, despite this decrease in AR mRNA expression, AR mRNA stability increases upon androgen stimulation and it is this increased mRNA stability that is thought to be responsible for the increase in AR protein levels. (7,17,19) It is also speculated that an increase in the cytoplasmic localization of AR mRNA due to HuR shuttling of the message and increases in the translational efficiency of the message by both HuR and PCBPs might also be partially responsible for the increase in AR protein levels. (7,15)

The regulation of AR mRNA by these RNA-binding proteins has the potential to have more significant implications in androgen-independent prostate cancer. The ability of these RNA-binding proteins to enhance AR protein formation and/or cause a more optimal distribution of AR protein within the cell can lead to an increase in the activation of the AR pathway and promote prostate cancer growth and advancement in an androgen-independent manner. (7)

The potentially significant role of AR mRNA regulation in prostate cancer progression makes this yet another potential target for therapeutic intervention in the fight against prostate cancer. (7,15) Due to the crucial part AR mRNA regulation might play in this disease, using molecular beacons to detect and track this mRNA in live cells could be incredibly useful in expanding our understanding of the development and progression of prostate cancer. (11-13)

1.4 Molecular Beacons for Live Cell mRNA Imaging

It has just been proposed that posttranscriptional regulation of AR mRNA by RNA-binding proteins could be responsible for the increased AR protein accumulation, subsequent pathway activation, and uncontrolled cell growth in some cases of androgen-dependent and androgen-independent prostate cancer. (7) The visualization of AR mRNA level, structure, and localization changes in androgen-dependent prostate cancer cells in response to hormonal induction and transition to androgen-independence could elucidate the importance of posttranscriptional regulation of this mRNA in promoting prostate cancer progression.

Molecular beacons, commonly used technology for real time RT-PCR product detection, have been shown to be useful in detecting mRNA in live cells. Molecular beacons are dual-labeled hairpin-structured oligonucleotide probes with a fluorophore at one end and a quencher at the other. The stem region on each side of the sequence complements to each other, holding the fluorophore and quencher together to prevent the emission of fluorescence and keep the beacon "silent". The hybridization domain, or "loop", is designed to be complementary to a specific mRNA target. When the mRNA target is present, the hybridization domain will bind to the target, opening the stem, displacing the fluorophore and quencher and allowing for fluorescence to be emitted upon excitation. A depiction of beacon structure and the change in conformation due to beacon-target binding is depicted in Figure 1. (21)

8
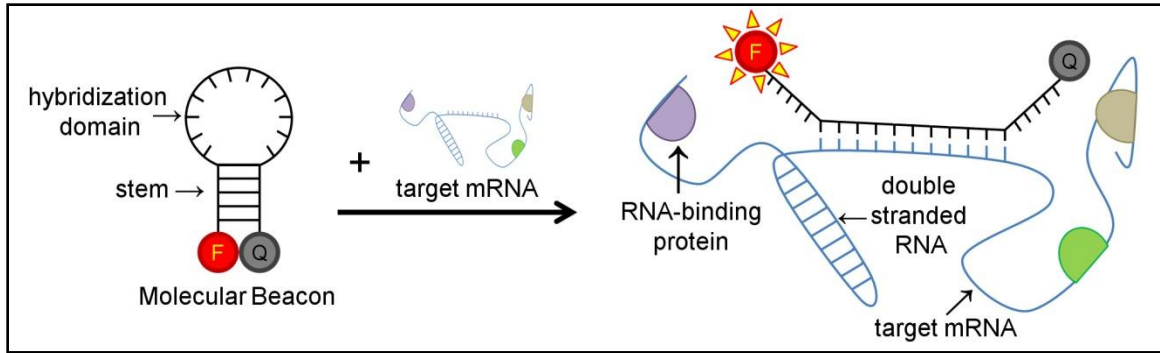
Figure 1: *Schematic of molecular beacon hybridization to target mRNA.* A molecular beacon is a dual-labeled hairpin oligonucleotide probe labeled with a reporter fluorophore at one end and a fluorescence quencher at the other end. Hybridization of the beacon with it's target mRNA opens the hairpin and separates the fluorophore from the quencher, allowing a fluorescence signal to be emitted. Site accessibility on the target mRNA can be an issue due to the secondary structure of the message and the presence of RNA-binding proteins that block sections of the oligonucleotide sequence.

The idea of the molecular beacon seems straightforward, but complications including target accessibility, probe specificity, and detection sensitivity are obstacles that researchers face when trying to employ this technology. Finding accessible sites on the target often involves the testing of multiple beacons targeted to different sites on the mRNA, which can be labor intensive. (11)

Enhancing detection sensitivity involves finding methods for increasing the signal-to-background ratio. One method that has been used is dual FRET molecular beacons, where two molecular beacons are designed to hybridize to neighboring sequences on the mRNA. One molecular beacon has a donor fluorophore, the other an acceptor fluorophore, and when the two beacons bind to the target, the donor fluorophore is able to excite the acceptor fluorophore. For live cell imaging, the donor fluorophore is excited and emission is collected in the optimal range for the acceptor fluorophore. Since two binding events are required for the acceptor fluorophore to fluoresce, it is less likely that

signal seen is from non-specific beacon opening, leading to an enhanced signal-to-background ratio. (12,13,22)

Another method for enhancing detection sensitivity is through the alteration of beacon backbone chemistry. Traditional beacons have an entirely DNA backbone. DNA-RNA interactions are not as strong as RNA-RNA interactions, so opening a DNA beacon to hybridize to an RNA target would not be as energetically favorably as an RNA beacon opening to bind to an RNA target. The switch to using 2'-*O*-Methyl (2'-*O*-Me) RNA chemistry, at least in the hybridization domain, enhances the thermodynamic favorability of beacon binding and the stability of the binding itself, leading to increased signal-to-background ratios. (11,23)

Molecular beacons have been used to detect several mRNAs in live cell assays. In our laboratory, live-cell detection of survivin (22,24), K-ras (13,22), GAPDH (13,24), and BMP-4 (11) mRNA, as well as the RNA virus Respiratory Syncytial Virus (RSV) (25,26), has been achieved. Live-cell detection of other mRNAs, such as β-actin mRNA (27,28), have also been reported in the literature.

1.5 Specific Aims

It was our goal to use a molecular beacon based approach to track AR mRNA in order to view mRNA expression, structure, and localization changes when prostate cancer cells undergo hormone stimulation of the AR growth pathway, changes in androgen sensitivity, and other stresses that affect the progression of the disease. We intended to use the information gathered through this technique to assess the importance of AR mRNA posttranscriptional regulation in prostate cancer progression.

The first aim of this project was to develop molecular beacons that target Androgen Receptor mRNA.   This aim was further divided into three sub-aims: A) design AR mRNA molecular beacons and determine their functionality, B) optimize the molecular beacon approach designed in sub-aim A, and C) validate the molecular beacon approach as specific for targeting AR mRNA.

First, beacons were designed based on previously established antisense sites and tested in solution for their integrity and in live cells to determine their ability to produce visible signal. Next, the beacons were optimized using two methods: 1) using multiple beacons in tandem and 2) changing beacon backbone chemistry. The optimized system was then validated using three different methods.   The first method of validation was to demonstrate the ability of the probe(s) to give a reasonable localization pattern. The second method was to show the ability of the probe(s) to distinguish between an AR+ and an AR- prostate cancer cell line, LNCaP and DU-145, respectively. The final method of validation was to alter the expression level of AR mRNA in either prostate cancer cell line and determine the ability of the probe(s) to follow changes in message level.

The second aim of this project was to use the AR mRNA targeted beacon(s) developed in the first aim to study the potential role of AR mRNA posttranscriptional regulation in two systems important in prostate cancer progression and development: 1) hormone induced androgen-dependent prostate cancer cell growth and 2) progression of prostate cancer cells from the androgen-dependent to the androgen-independent state.

Our model for studying hormone induced androgen-dependent prostate cancer cell growth was to treat the androgen-dependent prostate cancer cell line LNCaP with the

11

synthetic androgen R1881 and evaluate the effects using both comparative quantitative real time RT-PCR and AR mRNA visualization with molecular beacons. To study AR mRNA regulation differences between androgen-dependent and androgen-independent prostate cancer, we compared AR mRNA expression, structure, and localization in androgen-dependent LNCaP cells and androgen-independent LNCaP-derived C4-2 cells using our molecular beacon based approach.

If hormone stimulation of androgen-dependent prostate cancer cells produces a visible change in AR mRNA regulation, the ability to detect these changes could be enormously beneficial. By using molecular beacons to determine the androgen-induced changes in AR mRNA regulation in prostate cancer cells of an unknown state and comparing these results to those of known androgen-dependent prostate cancer cells, perhaps you could use this information as a diagnostic measure of whether or not the prostate cancer cells in question are still in the androgen-dependent phase. Also, by seeing how androgen-dependent prostate cancer cells typically respond to hormone stimulation, one could determine the ability of a therapeutic to disrupt typical AR mRNA regulation and impede this mechanism of cancer growth.

If there are characteristic changes in AR mRNA structure and localization that correspond with the transition of prostate cancer cells from androgen-dependent to androgen-independent, this method for visualizing AR mRNA could have potential diagnostic value in assessing the aggressiveness of the disease.

CHAPTER 2: METHODOLOGY

2.1 Beacon Design

Molecular beacons were designed to target a unique 16-20 nucleotide long sequence

within the AR mRNA transcript. A literature search was performed to find successful AR

mRNA antisense sites that could function as potential target sequences for our beacons.

Next, the selected nucleotide sequences were run through the National Center for

Biotechnology Information's (NCBI's) Basic Local Alignment Search Tool (BLAST) to

ensure that they were specific to AR mRNA.   Once the chosen target sequences were

verified as potential beacon hybridization domains, stem sequences were selected that

would allow the beacons to close in the classic hairpin structure in the absence of target

and have a reasonable melting temperature (in the range of 45-55°C). Next, Dr. Michael

Zuker's Mfold program for nucleic acid folding and hybridization prediction was used to

determine if our beacon would most probably take on the desired hairpin structure and

have an appropriate melting temperature. (29) Ensuring the beacons had an

appropriate melting temperature is important for avoiding beacon opening at physiologic

temperatures in the absence of target.   Mfold was run for our desired beacon

sequences at the physiologic temperature of 37°C and physiologic salt condition of

150mM NaCl. Once beacons were designed to meet all the criteria, their sequences

were sent to be synthesized with a Cyanine dye, Cy3, at the 5' end, and a quencher,

Black Hole Quencher 2 (BHQ2), at the 3' end. When the beacon folds into the hairpin

structure, the dye and quencher will be adjacent to each other and fluorescence will be

quenched. When the beacon hybridizes to its' target, the Cy3 dye will displace from the

quencher and fluorescence will be emitted. DNA Beacons were ordered from BioSource

International. Chimeric beacons were purchased Biosearch Technologies, Inc. and

Gene Link^{TM}.

13

2.2 Solution Testing of Molecular Beacons

All beacons were subjected to solution testing in order to ensure that they take on the proper hairpin conformation when not in the presence of their target sequence and open and fluoresce when in the presence of their target. Short synthetic DNA sequences that matched the beacon's target sequence were purchased from IDT, Inc.

Beacons were incubated at a concentration of 200 nM with or without their target sequence in 1x nuclease free PBS for 30 minutes at 37 °C. In samples containing the target sequence, the target was present at a concentration of 400 nM. The total incubation volume was 50 µL. The test was performed in triplicate and after incubation samples were placed in a black bottom 384-well plate and fluorescence levels were read in a Tecan Safire plate reader using 530 nm excitation with a 12 nm bandwidth and fluorescence was collected for the range of 560 to 600 nm with a 5 nm step size.

2.3 Cell Culture

LNCaP, C4-2, and DU-145 cell lines were generously given to us by Dr Leland Chung at Emory University. All three cell lines were grown in the following media formula: RPMI 1640 with L-Glutamine and Phenol Red (Gibco), 10% Characterized Fetal Bovine Serum (HyClone), and 1% 10,000 units/ml penicillin streptomycin (Invitrogen). Cells were passaged in tissue culture treated plastic T-75 filter top flasks using 1x PBS with calcium and magnesium (Sigma) and 0.5% trypsin-EDTA (Invitrogen).

For cell starvation, cells were placed into the following media formula, from here on referred to as starvation media: RPMI 1640 with L-Glutamine and without Phenol Red (Gibco). For certain treatments, including Vitamin D treatment, cells were placed in the following media formula, from here on referred to as depleted media: RPMI 1640 with L-

14

Glutamine and Phenol Red, 5% Charcoal/Dextran Treated Fetal Bovine Serum (HyClone), and 1% 10,000 units/mL penicillin streptomycin.

Cells treated and used for RNA isolation and subsequent comparative quantitative real time RT-PCR were plated at 30-50% confluency in 6-well tissue culture treated plastic plates (Corning, Inc. – Costar). 6-well plates were coated with 0.01% Poly-L-Lysine solution (Sigma) for 30 minutes at 37°C prior to the addition of cells to promote cell adherence.

Cells needed for imaging experiments were plated at 30-50% confluency in 2-chamber Lab-Tek II Chamber #1.5 German Coverglass System slides (Nunc). The chamber slides were pre-coated with Poly-L-Lysine using the same conditions as listed above.

2.4 RNA Isolation

Cells grown in 6-well plates were collected from the plate using 0.5% trypsin. The cells were pelleted using a microcentrifuge (Eppendorf Centrifuge 5402) at 2000 rpm and 4°C for 10 minutes. The cell pellet was washed with 1x PBS and repelleted at the same conditions. RNA was then isolated from the cell pellets using Ambion®'s PARIS™ kit without deviation from the product protocol.

2.5 cDNA Synthesis

cDNA synthesis was performed using Stratagene®'s Affinity Script™ Multi Temperature cDNA Synthesis kit loading 300ng of RNA per sample. The product protocol was followed explicitly, using Random Primers and the dNTP mix provided with the kit.

15

2.6 Comparative Quantitative Real Time RT-PCR

Comparative quantitative real time RT-PCR can be used to semi-quantitatively compare expression levels between samples by using the control sample's expression level as a reference (100% expression) and reporting experimental sample expression relative to this level (percentage of control's expression). Samples were prepared using Stratagene®'s Brilliant® SYBR® Green QPCR Master Mix and the samples were cycled and fluorescence measured using Stratagene®'s MX3005P Real Time PCR Machine.

AR was amplified using the following primers:

Forward – 5' CCTGGCTTCCGCAACTTAACAC 3' and

Reverse – 5' GGACTTGTGCATGCGGTACTCA 3', which produces a 168 base pair (bp) product. (30) β-actin was amplified using the following primers:

Forward – 5' ATGGGTCAGAAGGATTCCTATGTG 3' and

Reverse – 5' CTTCATGAGGTAGTCAGTCAGGTC 3', which produces a 359 bp product. (31) Samples were first denatured at 95 °C for 10 minutes, then run through 40 amplification cycles of 95 °C for 30 seconds, 58 °C for 60 seconds, and 72 °C for 90 seconds. Fluorescence levels were recorded at the end of each 58 °C annealing stage.

Comparative quantitative real time RT-PCR results are always reported in terms of AR mRNA expression level normalized by β-actin expression. Relative expression levels are always reported, meaning that the control group (always shown first in graph) is calculated to have an expression level of 1, and AR mRNA expression level for all treatment groups is reported relative to the control group. β-actin was explicitly selected as the normalizing housekeeping gene due to implications in the literature that GAPDH had variable expression levels among different prostate cancer cell lines. (32)

16

2.7 Intracellular Beacon Delivery

Molecular beacons were delivered using the Streptolysin O (SLO) based reversible permeabilization method. (11,13,22,24-26)   2 units/mL SLO was activated for 45 minutes at 37 °C with 10 mM Tris(2-carboxyethyl)phosphine (TCEP) hydrochloride (Sigma) at a final concentration of 10 mM.   50 µL of activated SLO was then added to 450 µL of media. Beacons were then added to this mixture at a final concentration of 750 nM. The beacon-SLO-media cocktail was then added to a well of the 2-chamber slide and the slide was placed in the incubator at 37 °C and 5% CO_2 for 10 minutes. The cocktail was then removed gently via a micropipettor and fresh media was added to the well. Cells were returned to the incubator for 30 minutes to allow time for beacon hybridization and then imaging was performed. Slides to be kept for later use were fixed with 4% nuclease-free paraformaldehyde for 10 minutes at room temperature and stored in 1x nuclease-free PBS at 4 °C.

2.8 Total RNA Staining

SYTO® RNASelect™ green fluorescent cell stain, a nonspecific RNA label from Molecular Probes™, was used to stain for the total RNA in live cells.   A 500 nM final concentration RNASelect™ solution was applied for 30 minutes at 37 °C. Cells were then washed in 1x PBS containing calcium and magnesium and placed back into regular media before imaging.

2.9 siRNA Transfection

A literature proven 21-nucleotide AR-targeted siRNA:
5' AAGCCCATCGTAGAGGCCCCA 3' was used to knockdown AR mRNA in LNCaP cells. The control siRNA used by this group was selected as well:

5' ACCCCGGAGATGCTACCCGAA 3' (Dharmacon®). (33) Multiple transfection

reagents were tested using the conditions listed in the following sections. RNA was

isolated or cells were imaged to view AR mRNA knockdown 48 hours post-transfection.

For all reagents, the starting conditions recommended by the manufacturer were tested.

For Lipofectamine™ 2000, optimization was performed and reported.

2.9.1 Lipofectamine™ 2000

Cells were plated in either 6-well tissue culture treated plates or 2-well chamber slides,

depending on whether they were used for RNA isolation or imaging experiments,

respectively. Cells were plated at least 24 hours before transfection and were 30-50%

confluent at the time of transfection.   Cells were transfected using a 1 µg siRNA: 4 µl

Lipofectamine™ 2000 ratio. For a 6-well plate transfection: siRNA was diluted to a final

volume of 250 µl using serum free RPMI 1640 media.   Lipofectamine™ 2000

(Invitrogen) was also diluted to a final volume of 250 µl using serum free RPMI 1640

media. Both the siRNA and Lipofectamine™ 2000 solutions were then incubated at

room temperature for 5 minutes, mixed, and incubated at room temperature for another

20 minutes. The solution was then added drop wise to a single well of the plate

containing 2 mL of fresh media.   This process was proportionally scaled down for use in

2-well chamber slides based on surface area (5:2).

2.9.2 X-tremeGENE

Cells were transfected at 30-50% confluency. For a 6-well plate transfection: 2 µg siRNA was diluted to a final volume of 100 µl using serum free RPMI 1640 media. 10 µl of X-tremeGENE reagent (Roche) was also diluted to a final volume of 100 µl using serum free RPMI 1640 media. Both the siRNA and X-tremeGENE solutions were then incubated at room temperature for 5 minutes, mixed, and incubated at room temperature for another 15 minutes. The solution was then added drop wise to a single well of the plate containing 1.8 mL of fresh media.

2.9.3 FuGENE® 6

Cells were transfected at 30-50% confluency. For a 6-well plate transfection: 3 µl of FuGENE® 6 reagent (Roche) was diluted to a final volume of 100 µl using serum free RPMI 1640 media and incubated for 5 minutes at room temperature. 2 µg siRNA was then added to the solution and incubated for 15 minutes at room temperature. The solution was then added drop wise to a single well of the plate containing 1.9 mL of fresh media.

2.9.4 Oligofectamine™

Cells were transfected at 30-50% confluency. For a 6-well plate transfection: 2.5 µg siRNA was diluted to a final volume of 180 µl using serum free RPMI 1640 media. 3 µl of Oligofectamine™ reagent (Invitrogen) was diluted to a final volume of 15 µl using serum free RPMI 1640 media. Both the siRNA and Oligofectamine™ solutions were then incubated at room temperature for 5 minutes, mixed, and incubated at room temperature for another 20 minutes. The solution was then added drop wise to a single well of the plate containing 1.8 mL of fresh media.

19

2.9.5 DharmaFECT® 3

Cells were transfected at 30-50% confluency. For a 6-well plate transfection: 2.5 µg siRNA was diluted to a final volume of 200 µl using serum free RPMI 1640 media and 6 µl of DharmaFECT3® reagent (Dharmacon®) was also diluted to a final volume of 200 µl using serum free RPMI 1640 media. Both the siRNA and DharmaFECT3® solutions were then incubated at room temperature for 5 minutes, mixed, and incubated at room temperature for another 20 minutes. The solution was then added drop wise to a single well of the plate containing 2.1 mL of fresh media.

2.9.6 Codebreaker™

Cells were transfected at 30-50% confluency. For a 6-well plate transfection: 8 µl of Codebreaker™ reagent (Promega) was diluted to a final volume of 625 µl using serum free RPMI 1640 media and incubated for 15 minutes at room temperature. 0.4 µg siRNA was then added to the solution and incubated for 20 minutes at room temperature. The solution was then added drop wise to a single well of the plate containing 2.4 mL of fresh media.

2.10 hAR Plasmid Transfection

hAR, a plasmid containing the full length coding region of human AR, was provided courtesy of Dr. Paul Rennie at the University of British Columbia. (34) The plasmid was used to upregulate AR mRNA in DU-145 cells. Transfection of these cells was performed using Roche's FuGENE® 6 Transfection Reagent. Cells were ~70-80% confluent at the time of transfection.   For a 6-well tissue culture treated plate transfection: 3 µl of FuGENE reagent was diluted to a final volume of 100 µl using serum free RPMI 1640 media and incubated for 5 minutes at room temperature. 1 µg hAR plasmid was then added to the solution and incubated for 15 minutes at room

20

temperature. The solution was then added drop wise to a single well of the plate containing 1.9 mL of fresh media. hAR plasmid effects were examined 2 days post-transfection. This process was proportionally scaled down for use in 2-well chamber slides based on surface area (5:2).

2.11 Vitamin D Treatment

Cells were plated in regular media for at least 24 hours before treatment and were not treated until 40-50% confluent. Active Vitamin D, 1α,25-dihydroxyvitamin D3, was used at a stock volume of 100 µM in ethanol (EtOH). For treatment, media was changed to depleted media, as described in section 2.3, and Vitamin D was added at a final concentration of 100 nM. An equal volume of EtOH was used to treat control cells. RNA isolation or imaging occurred 24 to 72 hours after treatment. (35)

2.12 Hormone Starvation Treatment

Cells were plated in regular media for least 24 hours before starvation treatment. Cells were approximately 30% confluent at the time of treatment. Cells were then placed in starvation media, as described in section 2.3, for a period of 1 to 12 days. The starvation media was changed out every other day to ensure the health of the cells.

2.13 Thapsigargin Treatment

Cells were plated in regular media for least 24 hours before beginning treatment. Thapsigargin was reconstituted at a stock concentration of 100 µM in dimethyl sulfoxide (DMSO). When cells were approximately 50-70% confluent, their media was changed to starvation media for a period of 16 to 20 hours, and then changed to depleted media containing a final concentration of 100 nM thapsigargin. An equal volume of DMSO was used to treat control cells. RNA isolation or imaging occurred 0 to 24 hours after

21

treatment. (36) It is important to note that we kept trials in the 24 hour time frame in order to avoid possible apoptotic side effects caused by thapsigargin, which typically occur between 2 and 7 days of treatment. (37,38)

Recovery of the cells was also performed by changing out the media on the cells to depleted media containing a volume of DMSO equivalent to the volume of thapsigargin used in the treatment. Recovery periods lasted 16 to 48 hours and RNA isolation or imaging was performed in this time frame.

2.14 Hormone Stimulation Treatment

Cells were plated in regular media for least 24 hours before beginning treatment. 1 µM synthetic androgen, R1881, in EtOH was a generous gift from our collaborator, Dr. Leland Chung, at Emory University. When cells were approximately 40-50% confluent, their media was changed to starvation media for a period of 16 to 20 hours, and then changed to fresh starvation media containing a final concentration of 10 nM R1881. An equal volume of EtOH was used to treat control cells. RNA isolation or imaging occurred 6 to 48 hours after treatment. This protocol was also a generous gift from Dr. Leland Chung at Emory University.

2.15 Intracellular Imaging

Early imaging experiments, including initial beacon optimization experiments, were conducted using the Zeiss LSM Meta 100 confocal microscope using 100x magnification. Images presented in the rest of this paper were primarily obtained using the Zeiss Axiovert 100 with a Zeiss 100x 1.3 numerical aperture (NA) oil lens and a Cooke Sensicam SVGA cooled charge-coupled device camera to capture the images. For molecular beacon imaging experiments, the Cy3 filter set was used with a 545 nm

22

excitation and 570 nm emission wavelength. Exposure times of 0.3 to 0.5 seconds were used to obtain the fluorescence images. A uniform exposure time was used for each experiment, including beacon signal optimization and AR mRNA regulation experiments. Exposure times were reduced gradually from 0.5 to 0.3 seconds for the optimization of the AR+ LNCaP vs. AR- DU-145 comparison. Images were false colored using the "black body" color map provided by Adobe Photoshop.

Experiments to quantify molecular beacon fluorescence intracellularly were performed on the Applied Precision Deltavision Core system with an Olympus 60x 1.42 NA oil lens and an HQ Cool Snap camera. Again, the Cy3 filter set was used and a uniform exposure time of 0.385 seconds was used for this set of experiments. Cells were imaged using 0.2 µm thick slices. Images were deconvolved and fluorescence was quantified using the softWoRx software package associated with the Deltavision Core system.

2.16 Quantification of Intracellular Molecular Beacon Signal

The softWoRx software package associated with the Deltavision Core system was used to quantify intracellular molecular beacon signal. Cells were selected individually and their total fluorescence per slice and maximum fluorescence value per slice were determined for all cellular slices.

The first characteristic that was determined per cell was average total fluorescence per 1 μm^3 cellular volume. The total fluorescence per slice for each cell was averaged, divided by the surface area of the cell, and divided through again by 0.2 µm to determine the average total fluorescence per 1 μm^3 cellular volume.   These values were then normalized by the average value of this characteristic for the control cells, giving control

23

cells an average value of 1 and the experimental group a relative value. This normalization allowed for the direct merging of several trials for each experiment without having to worry about delivery or other variations from trial to trial.

The second characteristic that was determined per cell was average maximum fluorescence value. The average maximum fluorescence value per slice of each cell was determined and then these values were normalized in the same manner as described above.

24

3.1 Design of Molecular Beacons

3.1.1 Beacon Design

Using two previously published works that "walked the gene" in order to determine accessible antisense sites on AR mRNA, two potential beacon sites were identified. (39,40) The first beacon designed was named AR-24, titled as such because it was based on the 24th region tested by one of the publications. (39) AR-24 is designed to hybridize to an 18 nucleotide sequence that is 1784 nucleotides from the start codon of the message. The target sequence was BLASTed to ensure that it was unique to AR mRNA and a stem sequence was chosen that gave the beacon an appropriate folding conformation at physiologic temperature. Figure 2 shows the nucleotide sequence of AR-24 along with a depiction of the folding conformation of the beacon at physiologic conditions of 37 °C and 150 mM NaCl.

AR-24: *5'- /Cy3/ CGAC CAATCATTTCTGCTGGCG GTCG /BHQ-2/ -3'*

ΔG = -1.87 kcal/mole

T_M = 53.7 ^{o}C

ΔH = -37.2 kcal/mole

ΔS = -113.8 cal/K·mole
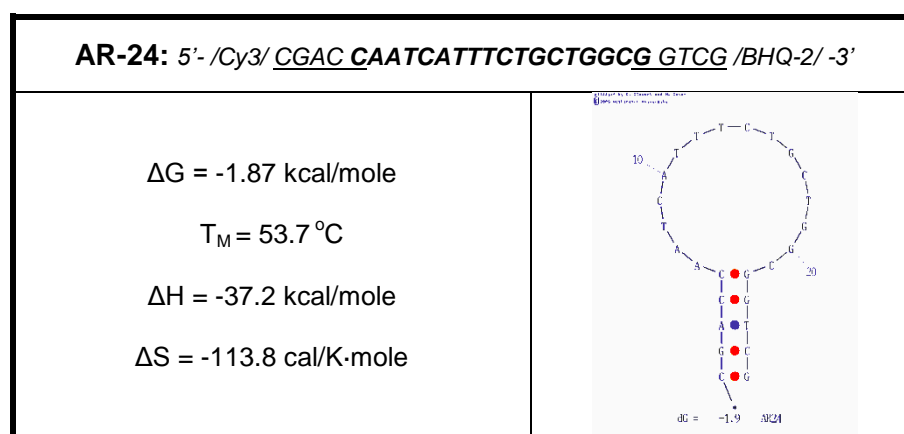
**Figure 2. *AR-24 DNA beacon for targeting AR mRNA.* The molecular beacon sequence is listed above. The underlined bases are part of the molecular beacon stem and the bolded bases are part of the hybridization domain. The thermodynamic properties of the beacon as calculated by Mfold are listed and an Mfold produced depiction of the beacon structure at physiologic conditions is presented. (29)

25

The second beacon designed was named AR-7, following the same naming convention.

AR-7 is designed to hybridize to an 18 nucleotide sequence that starts 1317 nucleotides

from the start codon. Again, the same rigorous analysis was preformed to ensure

uniqueness of the targeted sequence and an appropriate stem was chosen to allow for

proper hairpin conformation of the beacon. In figure 3, the nucleotide sequence of AR-7

is listed along with the folding conformation of the beacon.

AR-7: *5'- /Cy3/ <u>CCGTG</u> **ATACAACTGGCCTTCTTC** <u>CACGG</u> /BHQ-2/ -3'*

ΔG = -1.72 kcal/mole

T_M = 50.9 ^{o}C

ΔH = -39.5 kcal/mole

ΔS = -121.9 cal/K·mole
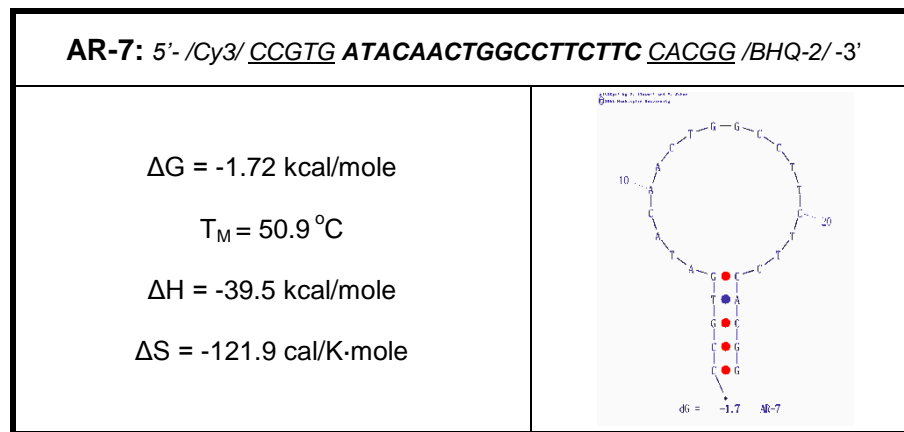
Figure 3. *AR-7 DNA beacon for targeting AR mRNA.* The molecular beacon
sequence is listed above. The underlined bases are part of the molecular beacon stem
and the bolded bases are part of the hybridization domain. The thermodynamic
properties of the beacon as calculated by Mfold are listed and an Mfold produced
depiction of the beacon structure at physiologic conditions is presented. (29)

3.1.2 Solution Testing of Beacons

Both beacons functioned as expected. Their fluorescence was quenched when the

beacon was not in the presence of target, with minimal noise detected at the Cy3

emission wavelength. Table 1 shows the signal-to-background ratio for each beacon at

Cy3's optimal emission wavelength, 570nm.

Table 1. *Signal-to-background ratio for AR molecular beacons at 570 nm.* The signal-to-background ratio was calculated by measuring the fluorescence emission at 570 nm for beacons exposed to target and then dividing by the fluorescence emission at 570 nm for beacons in the absence of target. The ratio was calculated in three independent trials and the average and standard deviation are reported for both AR-7 and AR-24.

	Signal-to-Background Ratio at 570 nm emission
AR-7	17.408 ± 0.812
AR-24	43.526 ± 3.081

3.1.3 Testing Molecular Beacons Intracellularly

Molecular beacons were introduced to cells using the Streptolysin O method discussed in section 2.7. Both beacons were tested individually in the AR+ prostate cancer cell line, LNCaP. In figure 4, the results of the preliminary test are shown indicating that the beacons do produce signal intracellularly. Whether this signal is specific will be explored in section 3.3. The next section will discuss the optimization the beacons to allow for maximal signal-to-background intracellularly.
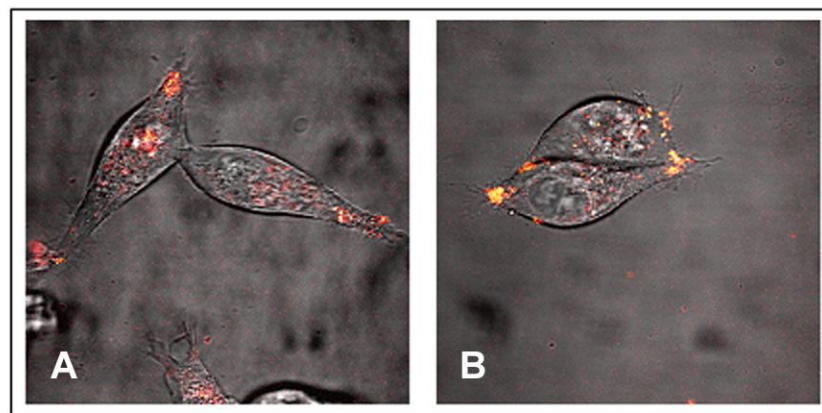
Figure 4. *AR-7 and AR-24 molecular beacon signal in LNCaP cells.* This figure shows LNCaP cells cultured in two-well glass chamber slides that have had A) AR-7 or B) AR-24 introduced via SLO permeabilization. White light and Cy3 fluorescence signals have been coregistered to show signal localization.

3.2 Optimization of Molecular Beacons

In section 3.1, the design of two potential AR mRNA targeted beacons, AR-7 and AR-24, were discussed. The solution study confirmed that these beacons folded properly, with minimum noise in the Cy3 channel and strong signal-to-background ratios when in the presence of their synthetic targets. In anticipation that the signal-to-background will greatly diminish when imaging the beacon signal intracellularly, two methods were explored for amplifying the signal-to-background ratio and these methods will be discussed in the following sections: 1) using multiple beacons in tandem and 2) modifications of the beacon backbone chemistry.

3.2.1 Using Multiple Beacons to Amplify Targeted Molecular Beacon Signal

The first method explored for amplifying the signal-to-background ratio when imaging AR mRNA intracellularly was the possibility of using both molecular beacons designed in tandem. Using the AR+ model prostate cancer cell line LNCaP, the two designed beacons, AR-7 and AR-24, were tested individually and in tandem to determine if the targeted signal could be boosted when multiple probes are hybridized to the same mRNA target. In figure 6 in section 3.2.2, images depicting the intracellular signal emitted from AR-7 individually, AR-24 individually, and the two beacons used in tandem are provided alongside with the results for enhancing signal-to-background using altered molecular beacon chemistry. The use of the beacons in tandem does appear to aid in amplifying the targeted signal, improving the signal-to-background ratio in the image.

3.2.2 Changing Beacon Backbone Chemistry

The second approach that was used to enhance the signal-to-background ratio for intracellular imaging of the beacons was to change the backbone chemistry of the molecular beacons. The beacons discussed in section 3.1 were designed with a

28

standard DNA backbone. Since we are targeting mRNA, the hybridization of these

beacons with target mRNA requires a DNA-RNA interaction. An RNA-RNA interaction

would be more energetically favorable for beacon-target binding and perhaps lead to a

greater amount of beacons binding to the target mRNA, thereby enhancing the signal-to-

background ratio in the intracellular imaging of these probes. Due to this theory, two

new molecular beacons were designed based on the hybridization domains of AR-7 and

AR-24. The new beacons, AR-7R and AR-24R, are chimeric beacons with 2'-*O*-Me

RNA bases in the hybridization loop of the beacons, and a maintained DNA stem holding

the beacon closed when in the absence of target. These new beacons will provide the

more energetically favorable RNA-RNA interaction for beacon-target binding by having

2'-O-Me RNA bases in the hybridization domain. The sequences for AR-7R and AR-

24R are listed below in figure 5. These beacons were also solution tested to ensure that

they still properly conformed and remained closed in absence of target.

AR-7R: *5'- /Cy3/ <u>CCGTGT</u> **AUACAACUGGCCUUCUUC** <u>ACACGG</u> /BHQ-2/ -3'*

AR-24R: *5'- /Cy3/ <u>CCTAC</u> **CAAUCAUUUCUGCUGGCG** <u>GTAGG</u> /BHQ-2/ -3'*

**Figure 5. *AR-7R and AR-24R: chimeric versions of AR-7 and AR-24 molecular
beacons.*** The molecular beacon sequences are listed above. The underlined bases
are part of the molecular beacon stem and the bolded bases are part of the hybridization
domain. Note that the bases in the hybridization domain are now 2'-*O*-Me RNA.

Direct comparisons between AR-7 and AR-7R, AR-24 and AR-24R, and AR-7 + AR-24

and AR-7R + AR-24R were performed in LNCaP cells to demonstrate the improvement

in signal-to-background that was achieved by modifying the backbone chemistry of the

probes. The results are depicted in figure 6. This figure also allows you to compare

signal from AR-7R to AR-24R and to AR-7R + AR-24R to further demonstrate the utility

of using multiple beacons in tandem as discussion in section 3.2.1. As is evidenced

29

from the representative images, use of both the beacons in tandem with the improved

chimeric backbone chemistry provided for the best signal-to-background in the

intracellular imaging of AR mRNA.
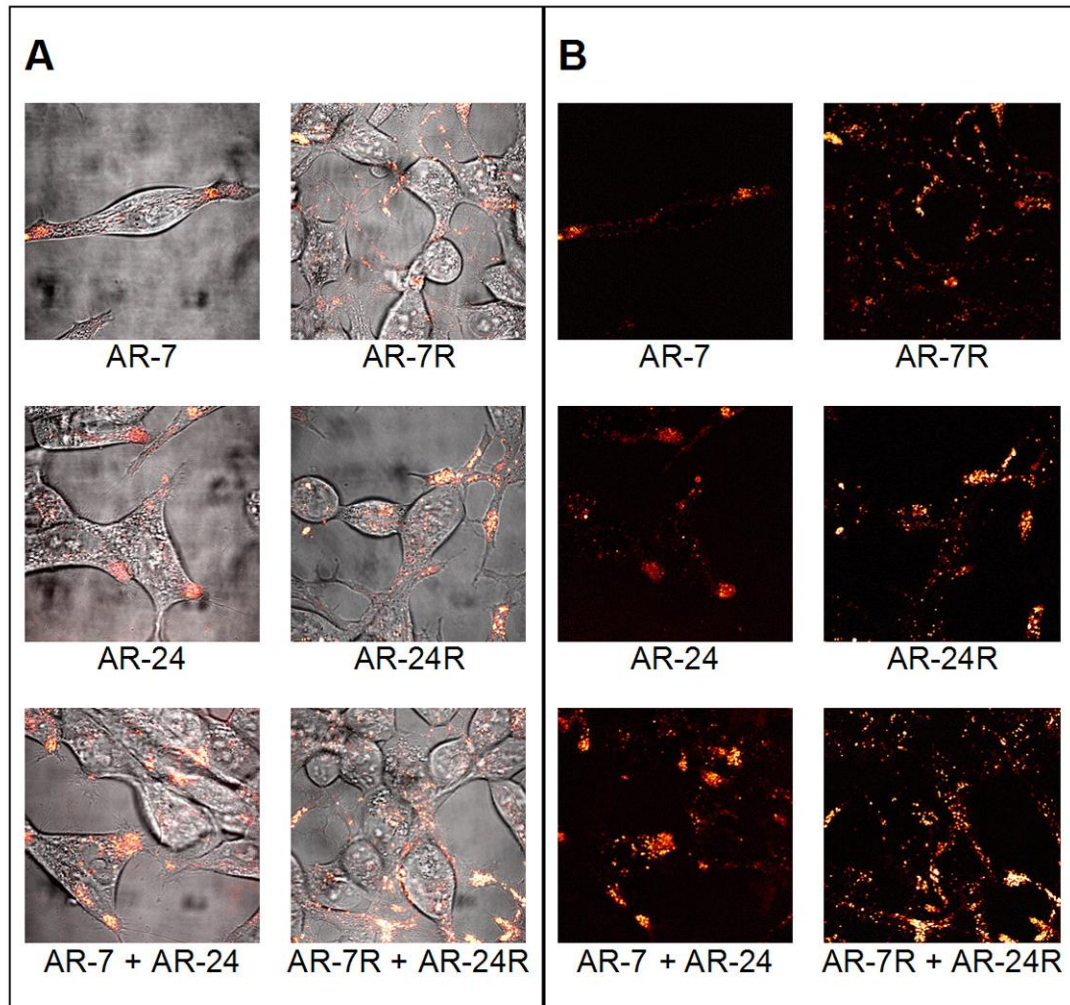
Figure 6. *Optimization of AR mRNA imaging through the use of multiple beacons in tandem and altering beacon backbone chemistry.* AR-7, AR-24, AR-7R, and AR-24R were introduced individually or in tandem to LNCaP cells in order to determine the value of using multiple beacons and the value of using the chimeric chemistry to boost beacon signal. All beacons were introduced at the same concentration and imaged at the same exposure conditions. Panel A shows the coregistration of the Cy3 fluorescence with the white light image to show cellular localization of signal. Panel B shows the Cy3 fluorescence alone to enable better comparison of the signal levels. By comparing AR-7 + AR-24 to both AR-7 alone and AR-24 alone or by comparing AR-7R + AR-24R to both AR-7R alone and AR-24R alone, the utility of using multiple beacons in tandem is evident. By comparing AR-7 to AR-7R, AR-24 to AR-24R, and AR-7 + AR-24 to AR-7R + AR-24R, the utility of changing to the chimeric chemistry is clear.

3.3 Validation of Molecular Beacons

3.3.1 Feasibility of AR mRNA Granular Pattern

There were several approaches used to prove that this optimized dual chimeric beacon system for tracking AR mRNA was in fact specifically binding to the desired target. The first approach was to determine the feasibility of the granular AR mRNA organization pattern being visualized through the use of the probe system. This determination of feasibility was achieved two ways: 1) total RNA staining to determine the typical localization patterns of RNA in the LNCaP model cell line and 2) an examination of the literature to determine if similar localization patterns for RNA have been see before and if proteins known to bind to this mRNA localize in this granular fashion.

LNCaP cells were stained with RNA select and their traditional RNA localization patterns are shown in figure 7. The localization pattern is granular in nature, which matches perfectly with the granular pattern that we see for AR mRNA using our probe system. Of course the total RNA stain shows many more granules than our probe system, which is also supportive of our system, because if our system is specifically labeling our desired target, then only a small subpopulation of the total cellular RNA should be labeled.

31
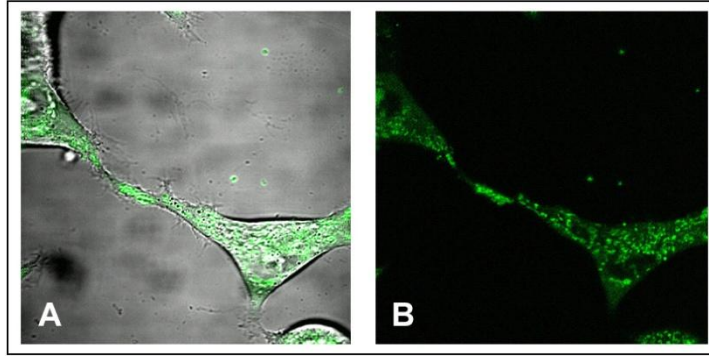
Figure 7. *RNA localization in LNCaP cells.* A nonspecific RNA Stain, RNASelect™, was used to visualize the general localization of mRNA in LNCaP cells. A) Shows a white light and green fluorescence coregistration to demonstrate cellular localization of the RNA. B) Shows the fluorescence image alone to more clearly articulate the granular structure of the RNA.

A granular RNA pattern has been seen before in the literature. Specifically, Dr. Robert Singer's group has demonstrated via Fluorescent In-Situ Hybridization (FISH) that β-actin mRNA has a granular pattern in fibroblasts and neurons. (41,42) Also, Dr. Jack Keene's group has shown Elav-Hu RNA-binding proteins known to colocalize with a family of mRNAs, including AR mRNA, organizing in a granular pattern in neurons. (43) But perhaps the most convincing piece of supporting evidence is that visualization of AR mRNA in the rat prostate gland using FISH also showed AR mRNA structure to be granular in nature. (44)

3.3.2 AR+ vs. AR- Prostate Cancer Cell Line Comparison

The next step for validating this probe system was to compare the beacon signal levels in an AR+ and an AR- prostate cancer cell line. Intracellular signal from the AR+ prostate cancer cell line LNCaP, which served as our model cell line for testing and optimizing our probes, was compared to the signal emitted from the AR- prostate cancer cell line DU-145. Figure 8 shows the intracellular signal levels in both cell lines using our optimized AR-7R + AR-24R probe system.

32
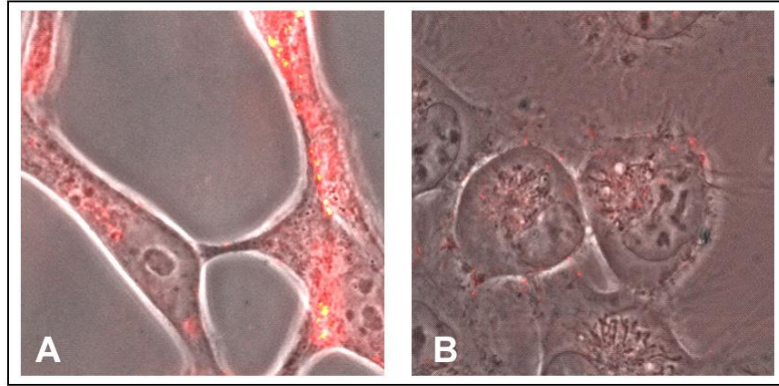
Figure 8. *Validation of dual chimeric beacon approach for visualizing AR mRNA using AR+ LNCaP vs. AR- DU-145 cell line comparison.* AR-7R and AR-24R were used in tandem and delivered to A) AR+ LNCaP cells and B) AR- DU-145 cells. The relatively low signal levels in the DU-145 cells compared to the LNCaP cells is an important observation in proving probe specificity.

In figure 9, you can see the progression of this AR+ vs. AR- cell line comparison as the probe system was optimized from a single DNA probe to two chimeric probes. The enhancement of signal to noise afforded by the optimized system allowed for reduction in image exposure time, permitting the AR+ vs. AR- cell line comparison to become increasingly more disparate.

33
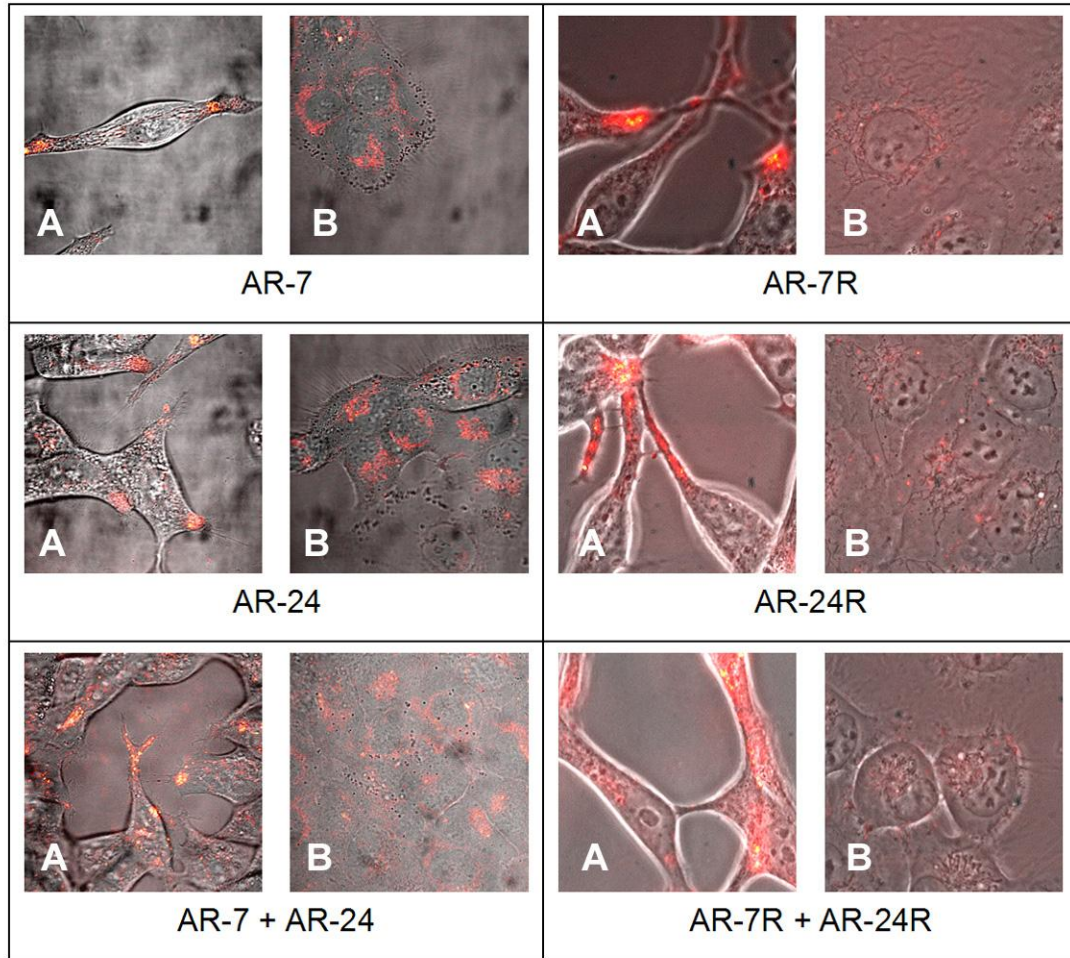
Figure 9. Demonstration of how dual chimeric beacon system affords more disparate comparison between LNCaP and DU-145 cell lines. AR-7, AR-24, AR-7R, and AR-24R were introduced individually or in tandem to A) LNCaP cells or B) DU-145 cells. Due to increased beacon signal intensity through the use of multiple beacons and chimeric backbone chemistry, it was possible to lower the image exposure time to allow the DU-145 cells to appear more "negative" while still showing strong positive signal from the LNCaP cells. Using the optimized dual chimeric system allowed for the most disparate comparison between the AR+ and AR- prostate cancer cells lines.

Total RNA staining was used to demonstrate that the typical organization of RNA in DU-145 cells does not agree with the faint signals seen from the AR molecular beacons. As seen in figures 8 and 9, the localization of the faint signals seen in DU-145 cells from AR molecular beacons is spotty and perinuclear. The total RNA staining of DU-145 cells in figure 10 shows that the general localization of RNA for this cell type is mitochondrial in

34

nature.   This leads us to believe that the beacon signal seen in DU-145 cells is non-

specific noise in the cell and not from beacons hybridizing to RNA.
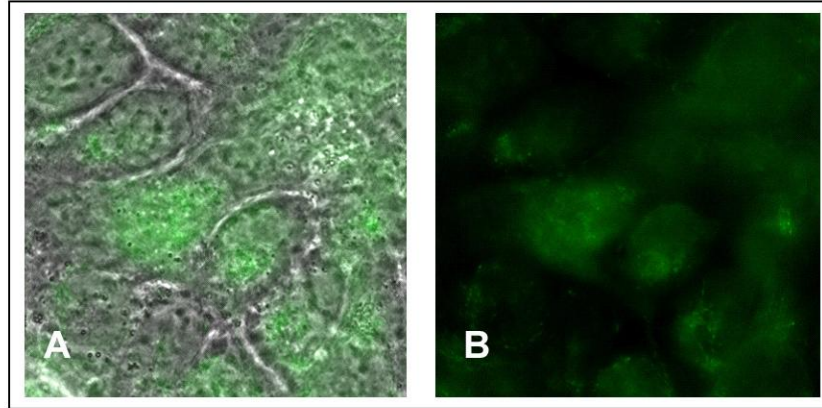
Figure 10. *RNA localization in DU-145 cells.* A nonspecific RNA Stain, RNASelect™, was used to visualize the general localization of mRNA in DU-145 cells. A) Shows a white light and green fluorescence coregistration to demonstrate cellular localization of the RNA. B) Shows the fluorescence image alone to more clearly articulate the mitochondrial localization of the RNA.

3.3.3 siRNA Knockdown of AR mRNA in AR+ Prostate Cancer Cell Line

The next approach attempted to validate AR mRNA targeted molecular beacons was to

take our model AR+ prostate cancer cell line, LNCaP, and induce significant knockdown

AR mRNA levels using siRNA. An AR siRNA sequence was selected from the literature

(33), and multiple transfection reagents were tested for their ability to induce AR mRNA

knockdown. Lipofectamine™ 2000 was the first transfection reagent tested. Figure 11

shows the knockdown achieved by Lipofectamine™ 2000 48 hours post transfection for

3 different concentrations of siRNA. The third transfection condition of 1.2 µg siRNA/mL

total volume was used due to its' repeatable high knockdown efficiency of ~85%. It is

important to consider that the knockdown level needs to be relatively high in order to

ensure the ability to visualize AR mRNA level changes due to the inherently low levels of

signal-to-background when imaging mRNA intracellularly.

35
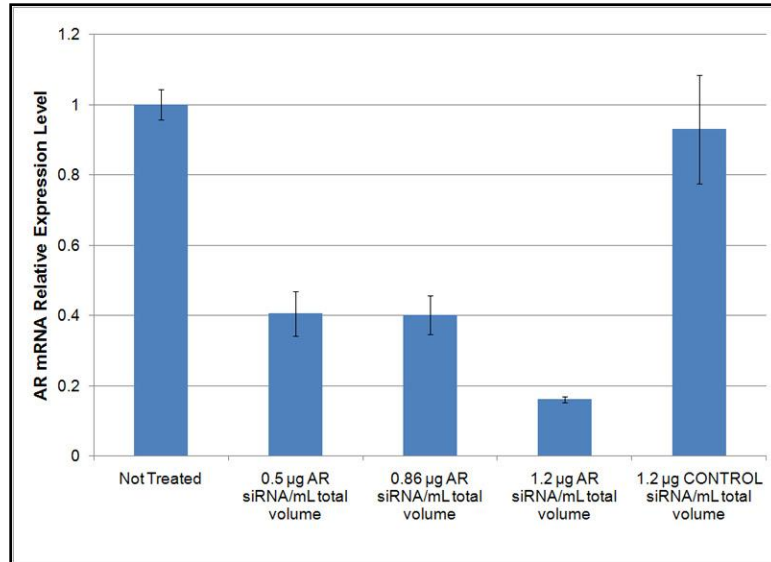
Figure 11. *AR mRNA knockdown in LNCaP cells using siRNA introduced via Lipofectamine*^{TM} *2000.* An AR mRNA specific siRNA was used to knockdown AR mRNA in LNCaP cells. Three different siRNA concentrations were tested, 0.5 μg/mL total volume, 0.86 μg/mL total volume, and 1.2 μg/mL total volume, with the highest concentration giving the best knockdown levels, 84.07 ± 0.77%. A control siRNA was used at the highest concentration in order to show that the knockdown effect was not nonspecific.

Once Lipofectamine^{TM} 2000 transfection conditions had been optimized, the siRNA

knockdown was performed on LNCaP cells and AR mRNA was detected using the dual

chimeric beacon approach. Figure 12 demonstrates the effects of the AR mRNA

knockdown using Lipofectamine^{TM} 2000 on AR mRNA targeted beacon signal.
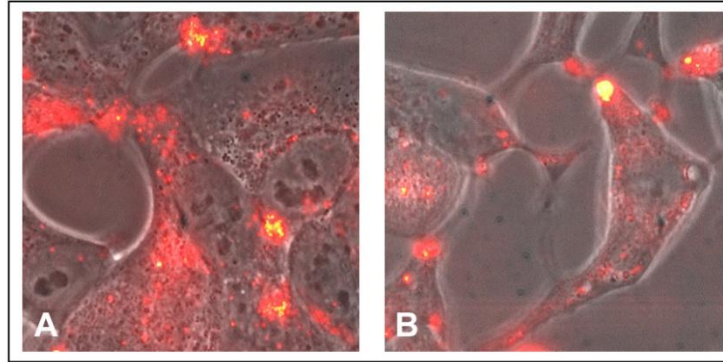
Figure 12. *Visualization of AR mRNA after siRNA induced knockdown via Lipofectamine^TM 2000.* AR mRNA was visualized using the dual chimeric beacon system. Signal levels in A) Non-treated LNCaP cells were compared with B) AR siRNA treated cells, 1.2 µg siRNA/mL total volume. In panel B, an overall drop in signal level could be argued, but the development of vesicles within the cell that often contain bright beacon signal was troubling.

As is evident from the images in figure 12, overall you might say that there is a diminishment of beacon signal in the siRNA treated LNCaP cells, however, there are large vesicles that have developed within the cell, presumably due to the transfection reagent. Lipofectamine^TM 2000's responsibility for the vesicle development will be shown later in this section when cells were exposed to a variety of transfection reagents without the presence of siRNA in order to determine the effect of the transfection reagents on LNCaP morphology. It appears that these large vesicles often colocalize with bright signal from the beacons (figure 13).
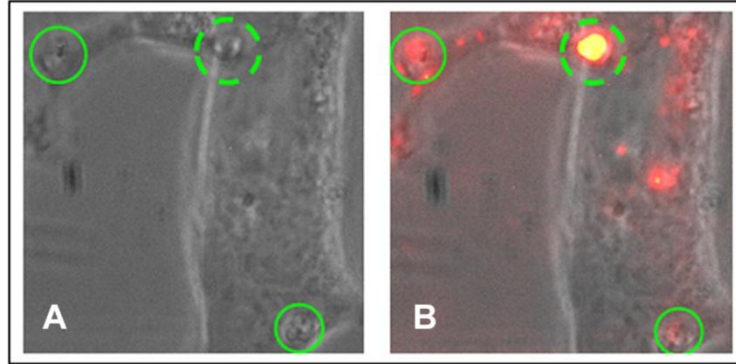
Figure 13. *Localization of AR beacon signal in Lipofectamine^TM 2000 delivered AR siRNA treated LNCaP cells.* AR mRNA was visualized using the dual chimeric beacon system. AR mRNA levels were knocked down in LNCaP cells via Lipofectamine^TM 2000 delivered AR siRNA, 1.2 μg/mL total volume. A) Shows a white light image of a treated LNCaP cell with the treatment induced vesicles circled in green. The vesicle that contained strong beacon signal is surrounded with a dashed green line. B) Shows the coregistration of the Cy3 fluorescence image with the white light image, indicating the presence of high fluorescence signal in the vesicle surrounded by the dashed green line. As is evident by the other circled vesicles, not all vesicles contain strong beacon signal. Some contain moderate to no beacon signal.

It is our hypothesis that these vesicles are trapping and degrading the beacons, but this would be extremely difficult to prove. However, the shear fact that this transfection reagent has such a profound effect on the cell morphology makes it difficult to believe that the signal level changes seen in the treated cells are truly indicative of AR mRNA level changes. It could be postulated that using cells treated only with Lipofectamine^TM 2000 would be a better control, but since the vesicle development occurs in that case as well, it would be difficult to ascertain whether or not there are true AR mRNA signal level changes when the cells have developed vesicles that appear to contain a large fraction of the beacons that have been introduced to the cells.

We felt it was important to use a system that does not have such a drastic effect on cell morphology for validating our probe system. We moved on to test the effects of several transfection reagents including FuGENE® 6, X-tremeGENE, Oligofectamine^TM, Codebreaker^TM, and DharmaFECT® 3 on both AR mRNA knockdown and cell

morphology. It was found that the mildest reagent on the cells in terms of changes to cell morphology was FuGENE® 6, but this reagent also had no effect on AR mRNA knockdown, making it a poor choice. Codebreaker™ also had limited effects on cell morphology and AR mRNA knockdown. X-tremeGENE caused considerable cell death with minimal effect on AR mRNA level and DharmaFECT® 3 also caused considerable cell death with moderate effect on AR mRNA level (~50% knockdown). Oligofectamine™ caused minimal changes to cell morphology and about 50% knockdown of AR mRNA. The effects of the different transfection reagents on AR mRNA knockdown and LNCaP cell morphology are shown in figures 14 and 15, respectively.
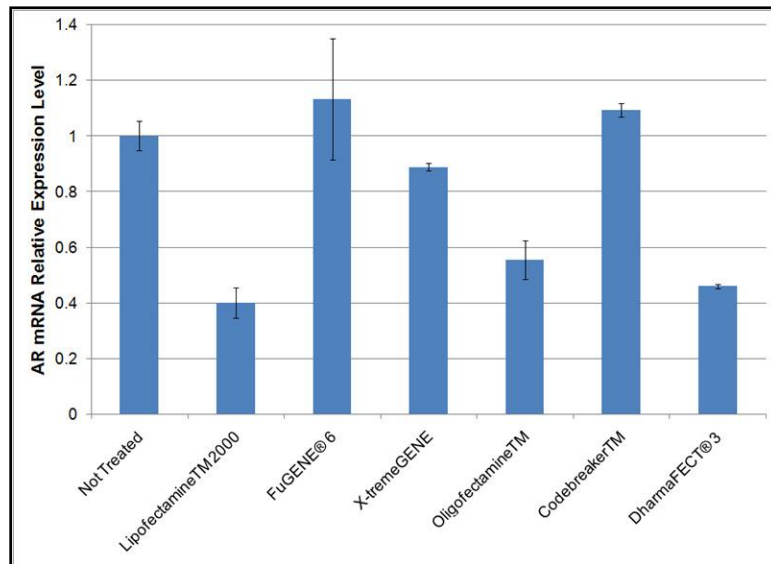
Figure 14. *siRNA induced AR mRNA knockdown using different transfection reagents.* Several transfection reagents were tested for their ability to knockdown AR mRNA, including: Lipofectamine™ 2000, FuGENE® 6, X-tremeGENE, Oligofectamine™, Codebreaker™, and DharmaFECT® 3. All reagents were tested at their initial manufacturer recommended conditions: Lipofectamine™ 2000 (0.86 μg siRNA/mL total volume), FuGENE® 6 (1 μg siRNA/mL total volume), X-tremeGENE (1 μg siRNA/mL total volume), Oligofectamine™ (1.25 μg siRNA/mL total volume), Codebreaker™ (0.133 μg siRNA/mL total volume), and DharmaFECT® 3 (1 μg siRNA/mL total volume). FuGENE® 6, X-tremeGENE, and Codebreaker™ provided for minimal to no AR mRNA knockdown. Lipofectamine™ 2000, Oligofectamine™, and DharmaFECT® 3 provided for at least 50% knockdown.

39
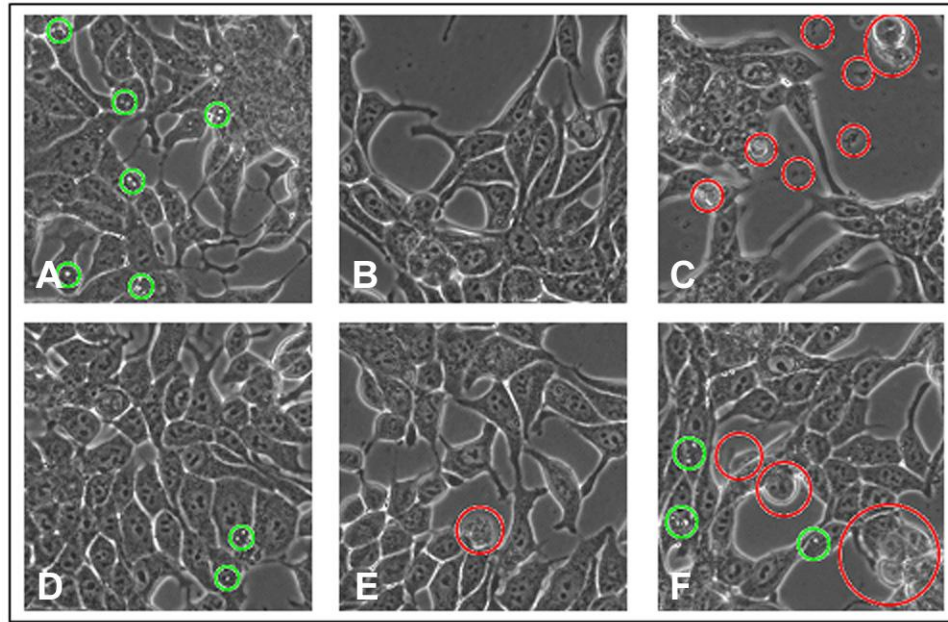
Figure 15. *LNCaP cell morphology changes due to siRNA transfection reagents.*
Several transfection reagents were tested to determine their effects on LNCaP cell
morphology. No siRNA was used in this experiment. The concentration of transfection
reagent used is described in section 2.9 and is identical to that used in the experiment
shown in Figure 14. LNCaP cells were visualized after treatment with the following
transfection reagents: A) Lipofectamine™ 2000, B) FuGENE® 6, C) X-tremeGENE, D)
Oligofectamine™, E) Codebreaker™, and F) DharmaFECT® 3. Green circles indicate
the development of intracellular vesicles, while red circles indicate the presence of dead
cells and cell debris. FuGENE® 6 caused the least change in cell morphology, followed
by Codebreaker™ and Oligofectamine™. However, of those three, only
Oligofectamine™ induced any AR mRNA knockdown.

Oligofectamine™'s ability to moderately knockdown AR mRNA with limited changes in

cell morphology encouraged us to attempt to optimize this reagent in order to get higher

levels of knockdown, while maintaining cell morphology, however, we were unsuccessful

(data not shown). At this point, using siRNA as a method for validating our probe

system was abandoned and other methods were pursued.

40

3.3.4 Upregulation of AR mRNA in an AR- Prostate Cancer Cell Line through the use of a Plasmid System

Due to the lack of success in modulating AR mRNA levels in the LNCaP cell line via siRNA, a second approach to modulate AR mRNA expression within the same cell line was explored. We attempted to upregulate AR in our AR- prostate cancer cell line model, DU-145, using a human Androgen Receptor (hAR) plasmid that was provided by Dr. Paul Rennie's lab at the University of British Columbia. (34) Fortunately, FuGENE® 6, which was shown to be the gentlest transfection reagent on cell morphology in the section 3.3.3, successfully delivered the hAR plasmid to DU-145 cells as shown via comparative quantitative real time RT-PCR in figure 16.
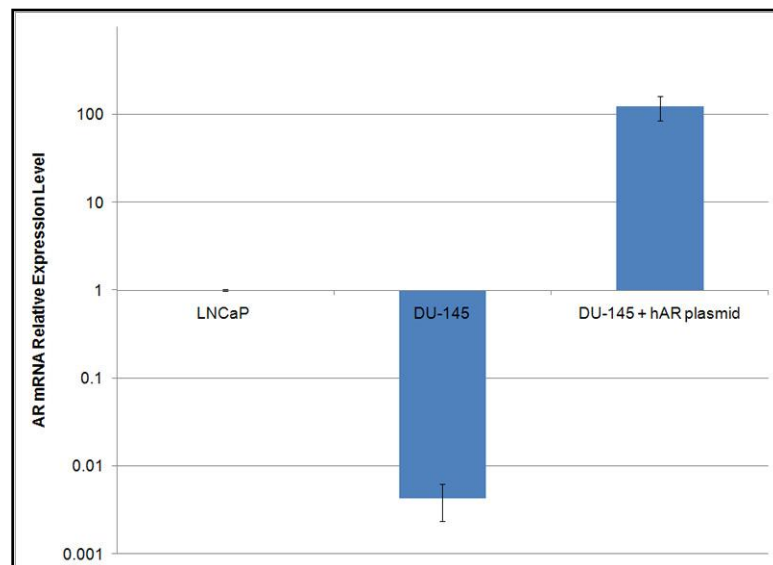
Figure 16. *Upregulation of AR mRNA in DU-145 cells using an hAR plasmid.* hAR plasmid was introduced to DU-145 cells by FuGENE® 6 to upregulate AR mRNA levels in this AR- prostate cancer cell line. AR mRNA levels rose to 122.07 ± 37.66 fold higher than that of the AR+ prostate cancer cell line, LNCaP. DU-145 AR mRNA levels are naturally over 230 times less than that of LNCaP cells, making it an AR- prostate cancer cell line.

Now that a method for upregulating AR mRNA levels in DU-145 cells had been established, the next step was to image the increase in AR mRNA expression using our

41

molecular beacon system. As you can see from figure 17, it was impossible to detect an

increase in AR mRNA beacon signal in DU-145 cells transfected with hAR plasmid.
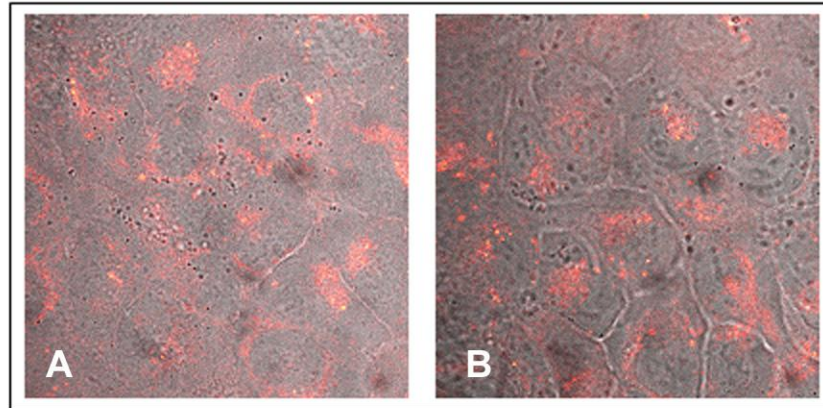
Figure 17. *Visualization of AR mRNA in DU-145 cells transfected with hAR plasmid.* AR mRNA was visualized using the non-optimized AR-7 + AR-24 DNA beacon system. Even with the non-optimized system, it is evident that you cannot see a difference between A) DU-145 cells and B) DU-145 cells + hAR plasmid, despite the dramatic increase in AR mRNA level afforded by the plasmid.

In order to determine if there was indeed some form of RNA being produced from the

plasmid, the general RNASelect™ stain was used to stain DU-145 cells that had been

transfected with the plasmid. As you can see from figure 18, the localization of the

mRNA in the hAR plasmid transfected cells contains large masses of RNA that do not

localize similarly to the endogenous RNA of the cell. Traditionally, DU-145 cells have a

mitochondrial localization to their RNA and these large masses do not fit in with this

pattern.

42
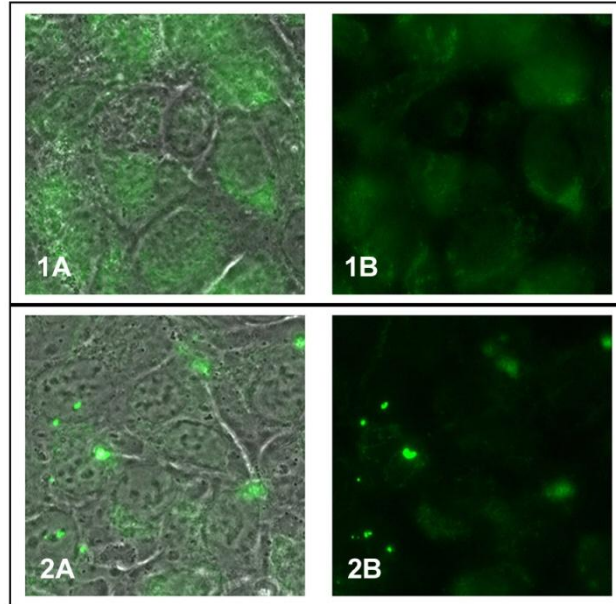
Figure 18. *RNA localization in DU-145 cells transfected with hAR plasmid.* A nonspecific RNA Stain, RNASelect™, was used to visualize the localization of all RNA in 1) DU-145 cells and 2) DU-145 Cells transfected with hAR plasmid. A) Shows a white light and green fluorescence coregistration to demonstrate cellular localization of the RNA. B) Shows the green fluorescence image alone to more clearly articulate the accumulation of large RNA globules in hAR plasmid-transfected DU-145 cells.

It was then speculated that since the plasmid did not contain the untranslated regions of

AR mRNA, the mRNA localization proteins that typically bind to AR mRNA were not

present, causing the AR mRNA produced to form an amorphous mass. It was also

probable that the AR mRNA produced from the plasmid did not take on the same

conformation as the endogenous AR mRNA due to the lack of the untranslated regions.

With an altered conformation, the accessible sites on AR mRNA will most likely be

different from what they are when the mRNA is in its' endogenous form, making sites

that were originally accessible to our beacons now inaccessible. The clustering of the

mRNA into a large mass and changes in site accessibility on the mRNA might make it

impossible for our beacons to hybridize to AR mRNA, making visualization improbable

with our probe system. Therefore, the inability of our beacons to detect the upregulation

of AR mRNA in DU-145 cells when they are transfected with hAR plasmid most likely is

43

not due to the beacons not accurately targeting AR mRNA, but rather due to the fact that the mRNA produced from the plasmid did not behave similarly to the endogenously produced mRNA.

3.3.5 Regulation of AR mRNA in an AR+ Prostate Cancer Cell Line via Indirect Signaling Methods

3.3.5.1 Upregulating AR mRNA by Vitamin D

It has been shown in the literature that Vitamin D can upregulate AR mRNA in LNCaP cells. (35,45) We attempted to harness this AR mRNA regulation method for validating our probe system. In figure 19, a time course for Vitamin D treatment was conducted in order to determine the optimal time point for maximal upregulation of AR mRNA. According to the literature, this time point should be 48 hours, and our results agreed with that time frame. The literature, however, showed a much higher maximal expression level, an 8 to 10-fold increase, than what we saw from this experiment, about a 2-fold increase. (35)
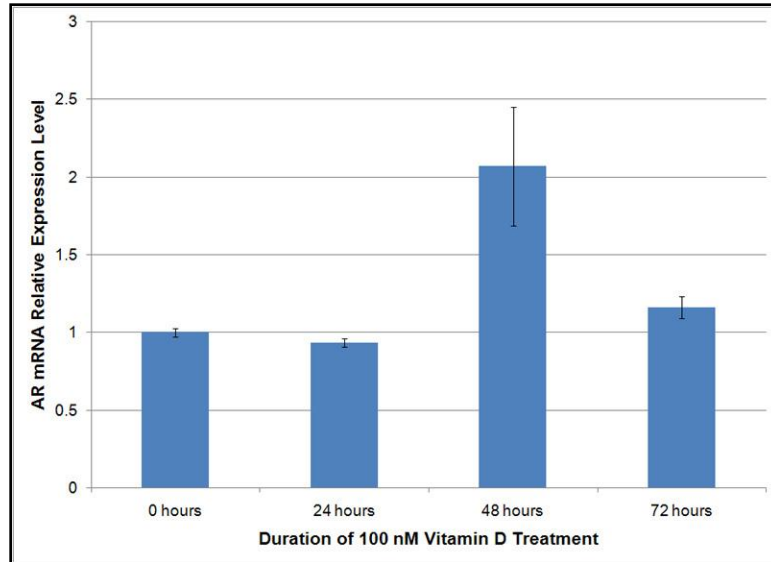
Figure 19. *Upregulation of AR mRNA in LNCaP cells using Vitamin D.* LNCaP cells were exposed to 100 nM Vitamin D treatment for a period 0, 24, 48, or 72 hours. AR mRNA relative expression level shows a 2-fold increase in AR mRNA expression level at 48 hours.

Considering the diminishment of the signal-to-background ratio when imaging the beacons intracellularly, there was concern that this minimal of an expression level change would be difficult to detect. In figure 20, AR mRNA was imaged in untreated and 100 nM Vitamin D treated cells using our dual chimeric beacon approach. It could be argued that there is slightly more intense signal in the Vitamin D treated cells, but the change is not drastic enough to be a convincing piece of proof towards probe specificity.

45
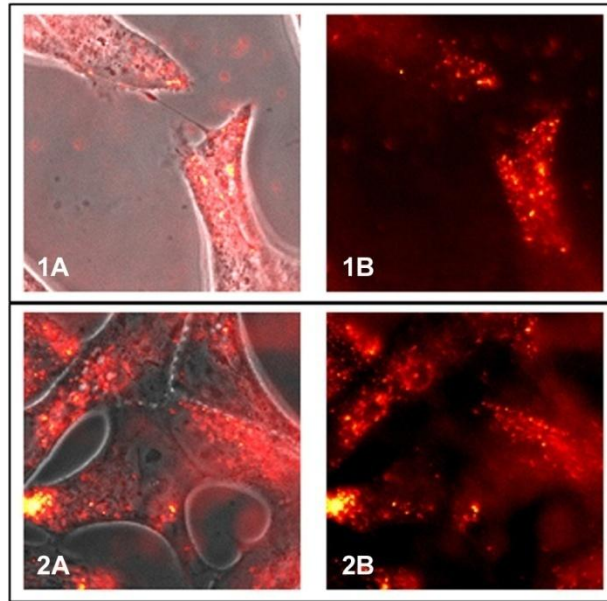
Figure 20. *Visualization of AR mRNA in LNCaP cells treated with 100 nM Vitamin D for 48 hours.* AR mRNA was visualized using the dual chimeric beacon system. LNCaP cells were either 1) not treated or 2) treated with 100 nM Vitamin D for 48 hours. A) Shows a white light and Cy3 fluorescence coregistration to demonstrate cellular localization of AR mRNA. B) Shows the fluorescence image alone to make the fluorescence level differences clearer. The difference between beacon signal level in non-treated versus Vitamin D treated LNCaP cells is not definitely discernible.

3.3.5.2 Upregulating AR mRNA by Hormone Starvation

A suggestion given to us by our collaborator at Emory University, Leland Chung, Ph.D. and by the literature, was to starve LNCaP cells from hormones for several days to induce the cells to upregulate their AR mRNA levels and stability in order to continue making AR protein. (16)   A time course was conducted to determine the increase in AR mRNA expression level over a course of 12 days of hormone starvation. The results of this time course are displayed in figure 21.

46
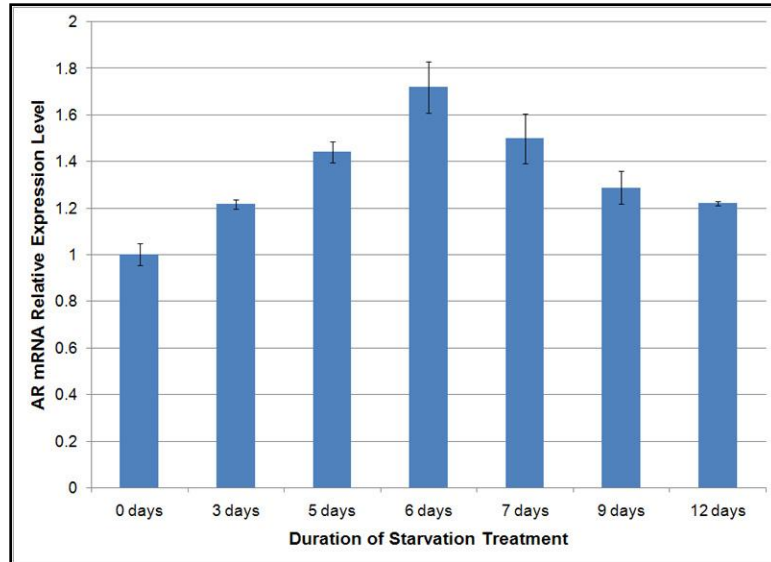
Figure 21. *Upregulation of AR mRNA in LNCaP cells via hormone starvation.*
LNCaP cells were incubated with starvation media, as described is section 2.12, for a period of up to 12 days. AR mRNA relative expression level was determined at 0, 3, 5, 6, 7, 9, and 12 days. AR mRNA levels reached their peak at 6 days, but the increased expression was less than 2-fold above the 0 day control.

As is evident from the results of the time course, AR mRNA levels rise until they peak at 6 days and then continue to drop off. At no point during the time course do levels rise above a 2-fold increase. Due to the difficulty in imaging the 2-fold increase induced by Vitamin D treatment, as discussed in section 3.3.5.1, this method was abandoned as a possible route for probe validation.

3.3.5.3 Downregulating AR mRNA by Thapsigargin

Gong et al. showed in 1995 that thapsigargin, a calcium ionophore, could be used regulate AR mRNA levels with precise temporal control. (36) Their work showed that after 100 nM thapsigargin was applied to LNCaP cells, the levels of AR mRNA decreased sharply until about 6 hours, and at 16 hours the levels began to recover. (36) We repeated this time course (figure 22) and determined that we could reach a maximal level of knockdown of ~80-85% between 6 and 16 hours post-treatment.

47
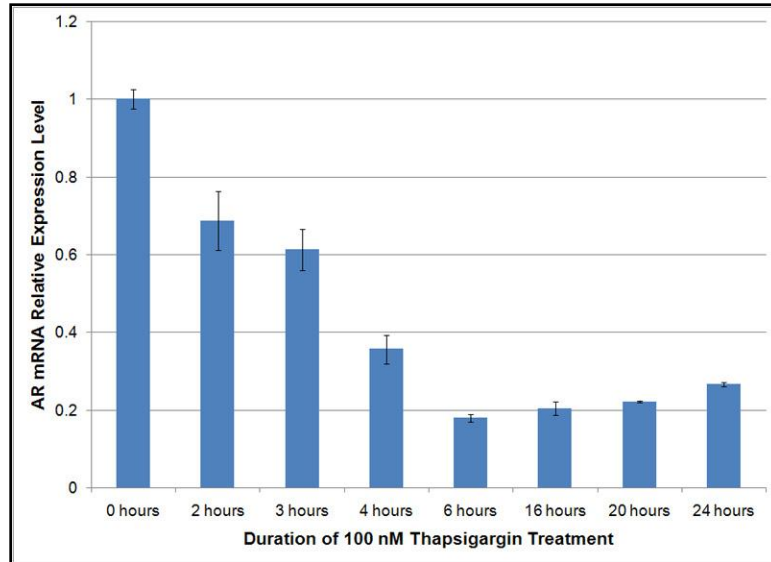
Figure 22. *Downregulation of AR mRNA in LNCaP cells using thapsigargin.*
LNCaP cells were exposed to 100 nM Thapsigargin treatment for up to 24 hours. AR
mRNA relative expression levels were determined at 0, 2, 3, 4, 6, 16, 20, and 24 hours
post-treatment. Maximal knockdown in AR mRNA expression was found to occur
between 6 and 16 hours of treatment, at a level between 80 and 85% knockdown.

The next step was to determine if we could visualize this drastic decrease in AR mRNA

level using our molecular beacons. The visual change might not be as striking as that

indicated with comparative quantitative real time RT-PCR, but the 5:1 to 10:1 control to

treated comparison should be detectable even with the reduced signal-to-background

afforded by epifluorescent imaging. As is seen in figure 23, the decrease in AR mRNA is

detectable with our dual chimeric beacon system.
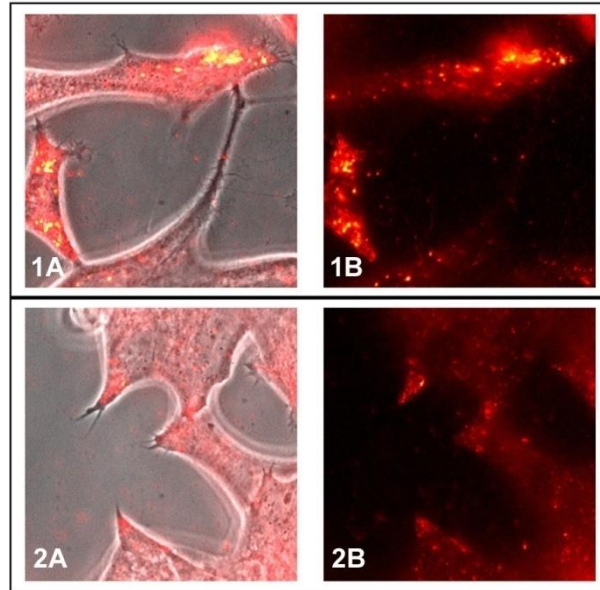
Figure 23. *Visualization of thapsigargin induced AR mRNA knockdown in LNCaP cells.* AR mRNA was visualized using the dual chimeric beacon system. LNCaP cells were either 1) not treated or 2) treated with 100 nM thapsigargin for 6 hours. A) Shows a white light and Cy3 fluorescence coregistration to demonstrate cellular localization of AR mRNA. B) Shows the fluorescence image alone to make the fluorescence level differences clearer. The difference between beacon signal level in non-treated vs. thapsigargin treated LNCaP cells is clearly visible.

The next step was to see if our beacons could detect the recovery of AR mRNA after thapsigargin treatment. LNCaP cells were treated with 100 nM thapsigargin for 6 hours and then their media was replaced and the cells were allowed to recover for 16-48 hours. The level of AR mRNA after 24 hours of recovery was to approximately 60% of the original level (figure 24).

49
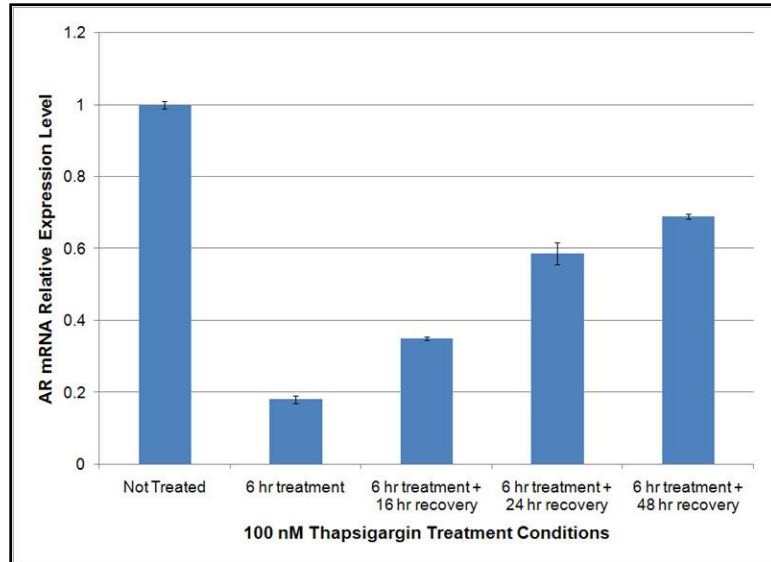
Figure 24. *Recovery of AR mRNA expression in LNCaP cells after thapsigargin treatment is removed.* LNCaP cells were exposed to 100 nM thapsigargin treatment for 6 hours and then their media was changed out to fresh media not containing thapsigargin. LNCaP cells were allowed to recover for a period of up to 48 hours and AR mRNA relative expression levels were determined after 16, 24, and 48 hours of recovery. At 24 hours of recovery time, AR mRNA levels had returned to $58.63 \pm 3.11\%$ of that of non-treated control cells.

This information indicates that the comparison of thapsigargin 6 hour treatment + 24 hour recovery to thapsigargin 6 hour treatment is about 3:1 to 6:1, which has a good probability of being visually detectable. However, the comparison of no treatment control to thapsigargin 6 hour treatment + 24 hour recovery is less drastic and might not be detectable. In figure 25, the intracellular visualization of these three points in this time course is presented. It is clear that you can see the recovery of AR mRNA signal in LNCaP cells after 24 hours of recovery time post-thapsigargin treatment. The visual confirmation that our probes can follow these temporal changes in AR mRNA adds to our argument that these beacons specifically target AR mRNA.
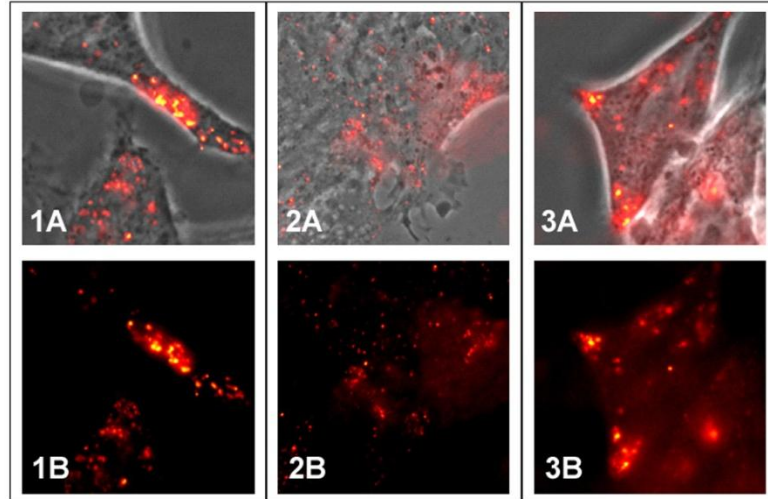
Figure 25. *Visualization of thapsigargin induced AR mRNA knockdown and post-treatment AR mRNA recovery in LNCaP cells.* AR mRNA was visualized using the dual chimeric beacon system. LNCaP cells were either: 1) not treated, 2) treated with 100 nM thapsigargin for 6 hours, or 3) treated with 100 nM thapsigargin for 6 hours and then allowed to recover for 24 hours. A) Shows a white light and Cy3 fluorescence coregistration to demonstrate cellular localization of AR mRNA. B) Shows the fluorescence image alone to make the fluorescence level differences clearer. The recovery of AR mRNA signal 24 hours after stopping thapsigargin treatment (Panel 3) is evident.

While the imaging was convincing in and of itself, we attempted to quantify the fluorescence levels within LNCaP cells at each phase of this thapsigargin time course. It was clear due to the limitations of signal-to-background with imaging that the changes we would see between the two groups would not be as drastic as those seen with our comparative quantitative real time RT-PCR results. It was unclear whether or not the difference between non-treated and recovered cells would be quantifiably detectable due to the minimal difference between these levels (less than 2:1). The difference between control and thapsigargin treated cells and the difference between thapsigargin treated cells and recovered cells would hopefully be able to be confirmed via fluorescence quantification due to their more drastic differences in expression level.

51

In figures 26 and 27, the quantification results are reported for both average total cellular fluorescence per unit of cellular volume and for average maximum fluorescence intensity per cell, respectively. As you can see, the thapsigargin treated cells have lower average total cellular fluorescence and lower maximum fluorescence than either the control or the recovered groups, but the difference between the control and the recovered group is indistinguishable on both counts. This is perhaps due to the limited difference in AR mRNA level between the two groups, less than 2:1. Overall, the changes seen through quantification are not nearly as drastic as those seen visually and through PCR. Possible reasons for the poor quantification results will be explored in Chapter 5.
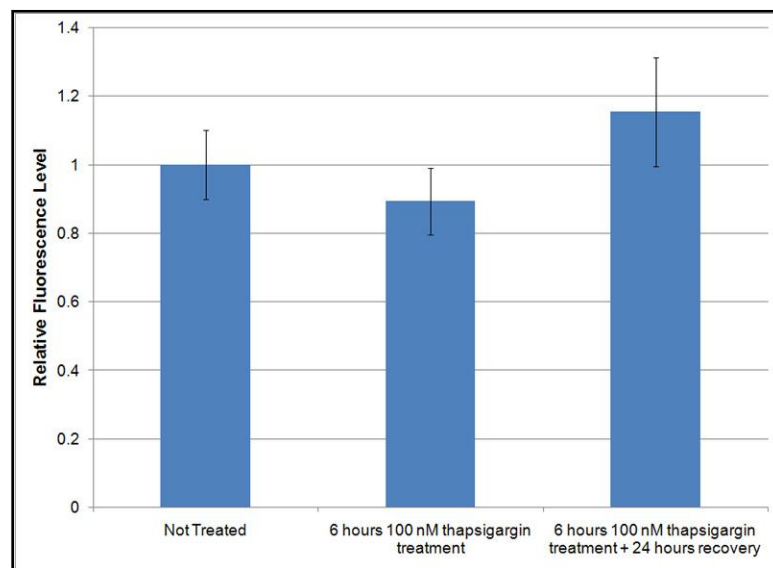
Figure 26. *Quantification of average AR beacon fluorescence per 1 µm^3 cellular volume in non-treated, thapsigargin treated, and post-thapsigargin treatment recovered LNCaP cells.* Non-treated, 100 nM thapsigargin 6 hour treated, and 100 nM thapsigargin 6 hour treated + 24 hour recovered cells were all incubated with the dual chimeric beacon system to allow for AR mRNA visualization. Using the softWoRx software package, average fluorescence per 1µm^3 cellular volume was calculated for a series of cells in each treatment group. Their values were averaged and normalized by the average value of the control non-treated group. Relative fluorescence levels for these three treatment groups are reported above. The 100 nM thapsigargin 6 hour treatment group did have lower fluorescence levels, and a recovery of fluorescence for the 100 nM thapsigargin 6 hour + 24 hour recovery treatment group was observed. However, the changes in fluorescence are not significant and are not nearly as dramatic as the comparative quantitative real time RT-PCR and the visualization results.

52
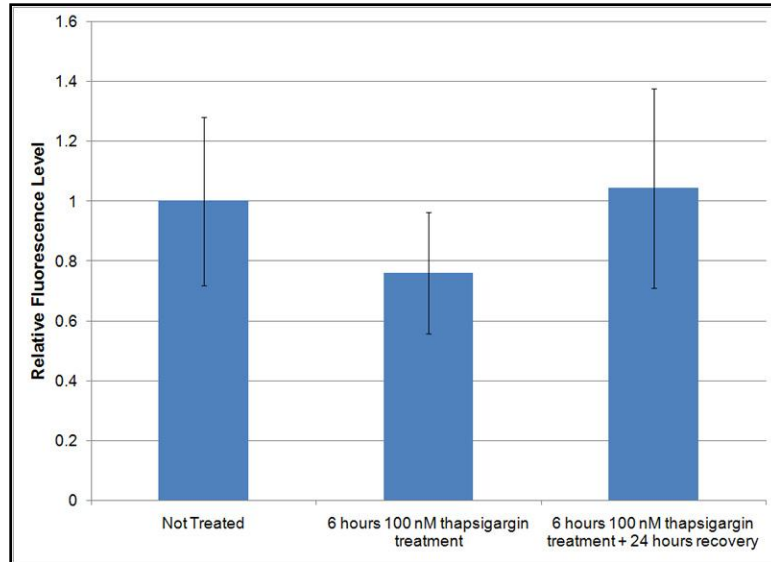
Figure 27. *Quantification of average maximum AR beacon fluorescence per cell in non-treated, thapsigargin treated, and post-thapsigargin treatment recovered LNCaP cells.* Non-treated, 100 nM thapsigargin 6 hour treated, and 100 nM thapsigargin 6 hour treated + 24 hour recovered cells were all incubated with the dual chimeric beacon system to allow for AR mRNA visualization. Using the softWoRx software package, average maximum fluorescence per cell was calculated for a series of cells in each treatment group. Their values were averaged and normalized by the average value of the control non-treated group. Relative fluorescence levels for these three treatment groups are reported above. Again, the 100 nM thapsigargin 6 hour treatment group did have lower fluorescence levels, and a recovery of fluorescence for the 100 nM thapsigargin 6 hour + 24 hour recovery treatment group was observed. But just as before, the changes in fluorescence are not significant and are not nearly as dramatic as the comparative quantitative real time RT-PCR and the visualization results.

Overall, the thapsigargin time course proved a useful tool for proving the specificity of our dual chimeric beacon approach for targeting and tracking AR mRNA, but the method of fluorescence quantification needs to be investigated to hopefully provide more convincing results.

CHAPTER 4: UTILIZING ANDROGEN RECEPTOR mRNA TARGETED MOLECULAR BEACONS TO STUDY POSTTRANSCRIPTIONAL MECHANISMS INVOLVED IN PROSTATE CANCER PROGRESSION

4.1 Studying AR mRNA Posttranscriptional Regulation Changes in AR+ Androgen-Dependent Prostate Cancer Cells Responding to Hormone Stimulation

In its' earlier stages, prostate cancer responds to hormone stimulation by the androgens testosterone and DHT. The ability of androgens to promote prostate cancer cells to continue growing and dividing is the principal reasoning behind using androgen ablation therapy as a treatment for prostate cancer. The hope is that by removing the stimulus, any prostate cancer cells left after surgery will no longer be promoted to grow.

As was stated in the section 1.1, testosterone works to promote prostate cancer cell growth by being transported inside the cell, converted to DHT, binding to Androgen Receptor, and then this complex dimerizes and moves into the nucleus where it acts as a transcription factor. One of the downstream targets that this transcription factor regulates is Androgen Receptor itself, allowing for the effect of testosterone to be further amplified by increasing the number of available Androgen Receptors for DHT to occupy. This positive feedback loop will continually drive the growth and division of these cells. (1)

The mechanism of this positive feedback loop is not completely understood, and what is understood about it is not intuitive. When androgen-dependent prostate cancer cells are exposed to DHT or synthetic androgens such as R1881, the level of AR mRNA decreases, but the mRNA has increased stability and greater protein production potential. (7,16-20) We wanted to determine if you could visualize androgen-induced AR mRNA posttranscriptional changes in androgen-dependent prostate cancer cells. If this

المنارة للاستشارات

www.manaraa.com

was possible, determining if prostate cancer cells exhibit these changes in response to hormone stimulation could be used indicate whether or not these cells are still in the androgen-dependent phase.

First we conducted a time course of LNCaP exposure to 10 nM R1881 for 48 hours to see the temporal response to the hormone in order to determine the time frame when the cells are responding to the hormone by downregulating AR mRNA (Figure 28). Based on this time course, the cellular response of AR mRNA downregulation appeared to occur at 24 hours post-hormone stimulation. The initial rise in AR mRNA was not seen in the literature previously (17), and should be repeated, but the decrease at 24 hours to about 50% of the control levels has been observed before. (16-18)
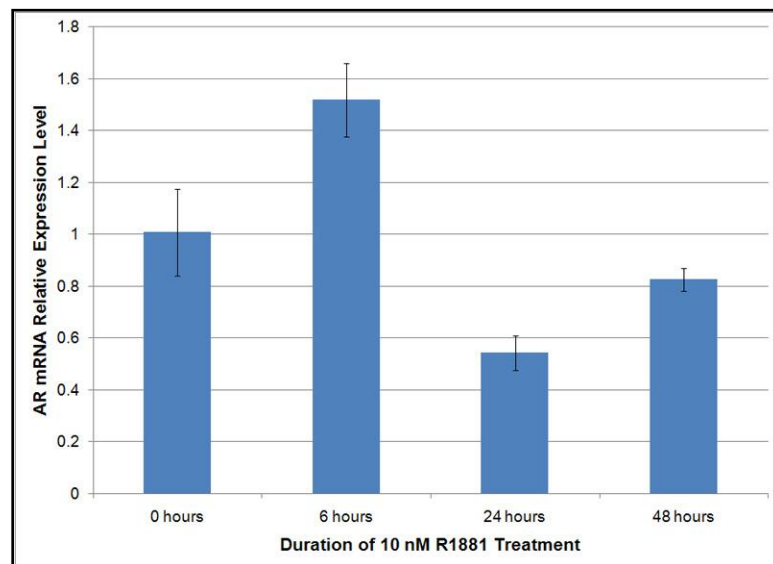
Figure 28. *Regulation of AR mRNA expression in LNCaP cells treated with 10 nM R1881.* LNCaP cells were exposed to 10 nM R1881 for a period of up to 48 hours. AR mRNA relative expression levels were determined at 0, 6, 24, and 48 hours post-treatment. At 6 hours, AR mRNA levels increased, with a sharp decline at 24 hours, and recovery towards control levels at 48 hours.

Next we wanted to see if there were visible changes in the AR mRNA structure and localization that corresponded to this R1881-induced posttranscriptional regulation. In figure 29, you can see that after 24 hours of R1881 exposure, the AR mRNA appears to cluster into larger granules. Whether or not this clustering plays a role in the stabilization and increased translational efficiency of this mRNA is yet to be determined.
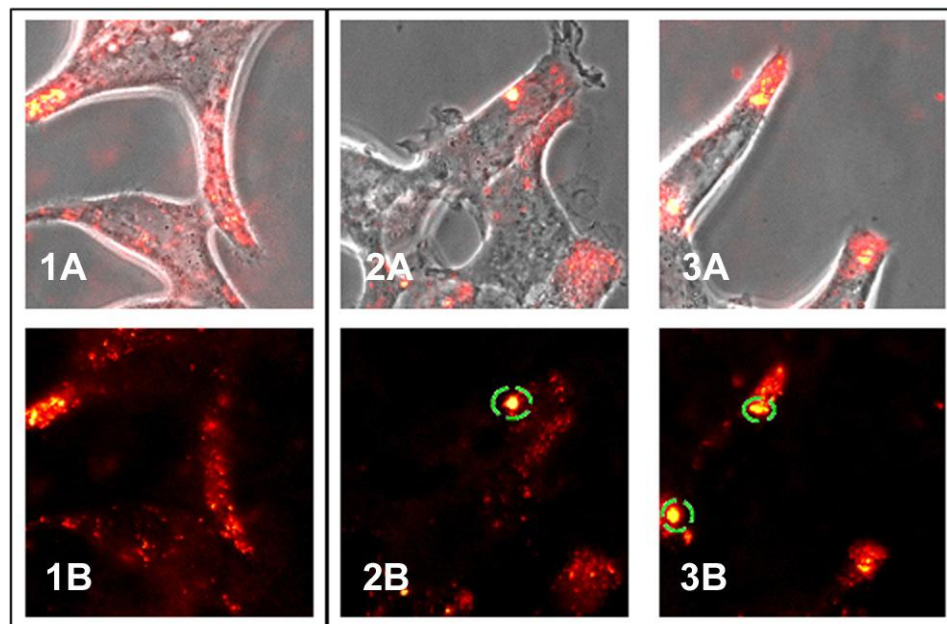
Figure 29. *Visualization of AR mRNA in LNCaP cells treated with 10 nM R1881 for 24 hours.* LNCaP cells were either 1) not treated or 2) and 3) treated with 10 nM R1881 for 24 hours. A) Shows white light and Cy3 fluorescence coregistration to demonstrate cellular localization of AR mRNA. B) Shows the fluorescence image alone to clearly show the structural changes in AR mRNA. 2B) and 3B) have green dashed lines surrounding significantly large mRNA granules that have developed after 24 hours of R1881 treatment.

4.2 Studying AR mRNA State Changes Associated with the Transition of Prostate Cancer from Androgen-Dependent to Androgen-Independent

When a tumor becomes androgen-independent, it no longer requires normal physiologic levels of testosterone to continue to grow and divide; it can survive and perpetuate at basal hormone levels. Often this ability to survive in low levels of androgen is due to

56

increased levels or optimized distribution of AR protein within the cell so that all available testosterone will occupy receptors and form active transcription factors.

Again, AR mRNA's role in this process is counterintuitive because if you had a tumor that could continue to grow in low levels of testosterone, you would assume that AR mRNA was upregulated in these tumors to drive the production of AR protein. However, the opposite is the case. As reported in figure 30, AR mRNA levels in the LNCaP-derived androgen-independent counterpart cell line, C4-2, is about 50% of that of the LNCaP level. Dr. Peter Leedman's group believes that differential posttranscriptional regulation of AR mRNA in androgen-independent cells drives either the accumulation or optimized distribution of AR protein despite the lowered message levels. (7,15,17) In the case of C4-2 cells, their lowered message levels are accompanied by lower AR protein levels, so in this case, changes in posttranscriptional regulation that lead to a more efficient distribution of the protein within the cell might be at play. (46)
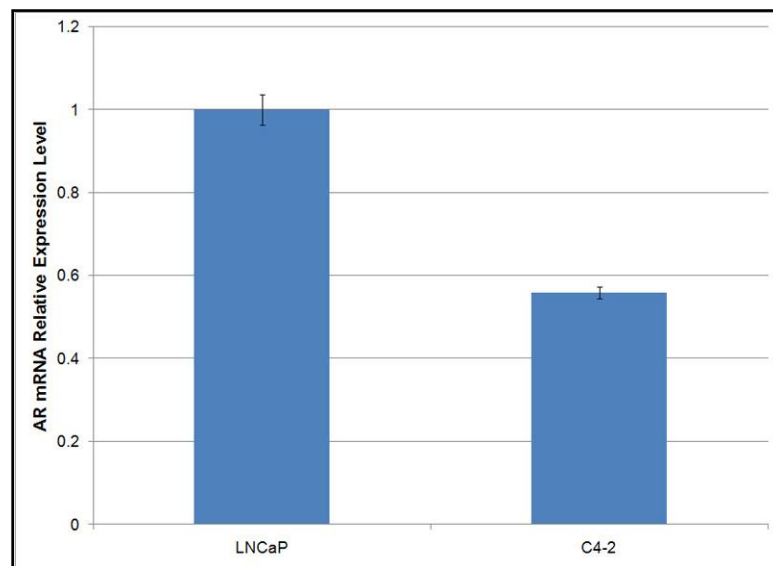
Figure 30. *Differences in AR mRNA expression between LNCaP and C4-2 cells.*
AR mRNA relative expression levels are presented for LNCaP cells and their androgen-independent counterpart cell line, C4-2. C4-2 AR mRNA levels are determined to be 55.87 ±1.34% of that of LNCaP cells.

57

We were curious if AR mRNA posttranscriptional regulation involved in driving the cell from the androgen-dependent to the androgen-independent state produced a visible change that you could use as a prognostic indicator of when a cell has made that crucial transition. To determine if this was the case, we used our model androgen-dependent cell line, LNCaP, and its' hormone starvation-derived androgen-independent counterpart cell line, C4-2, for a head-to-head comparison for determining if differential posttranscriptional regulation between the two cell lines caused a visible AR mRNA state change. In figure 31, you can see that the traditional AR mRNA granular pattern in LNCaP cells is altered when the cells are transformed to the C4-2 form. AR mRNA in C4-2 cells is granular in structure, but the pattern of the message is more dispersed throughout the cytoplasm. It is unknown whether or not this obvious localization change could be used for prognostic purposes.
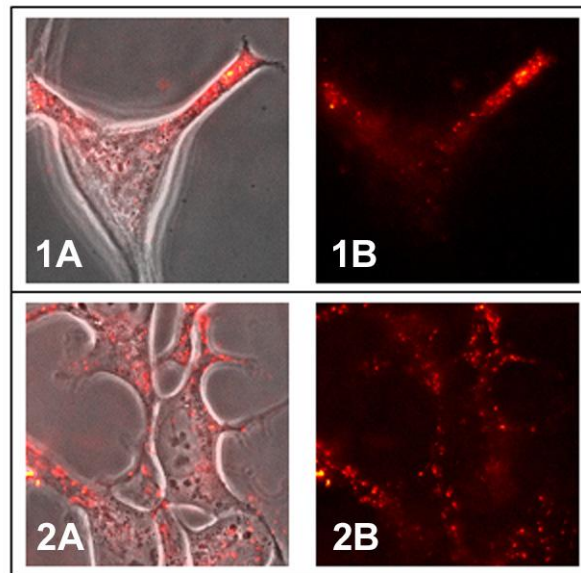
Figure 31. *Visualization of AR mRNA in LNCaP and C4-2 cells.* AR mRNA was visualized using the dual chimeric beacon system in 1) LNCaP cells and 2) C4-2 cells. A) Shows white light and Cy3 fluorescence coregistration to demonstrate cellular localization of AR mRNA. B) Shows the fluorescence image alone to clearly show changes in AR mRNA localization. In 1) LNCaP cells, AR mRNA granules are localized

58

more towards the edges of the cells, in structures we have termed "arms", while in 2) C4-2 cells, AR mRNA granules are dispersed more uniformly throughout the cytoplasm.

59

CHAPTER 5: DISCUSSION AND FUTURE DIRECTIONS

This thesis has presented a method for tracking AR mRNA in live prostate cancer cells using dual-labeled hairpin oligonucleotide probes known as molecular beacons. Two potential beacons, AR-7 and AR-24, were designed, tested in solution, and then tested in an AR+ prostate cancer cell line, LNCaP, to demonstrate their potential capability of allowing for AR mRNA visualization in live cells.

The localization pattern of AR mRNA in AR+ LNCaP cells seen using these AR mRNA targeted molecular beacons was interesting in and of itself. It appears that the message localizes predominantly in granules in the extremities or "arms" of the cells. Localization of mRNA to leading edges of a cell has been seen before, further validating this pattern as a feasible result. Dr. Robert Singer's group observed the same subcellular localization for β-actin mRNA in fibroblasts and neurons. Singer also observed that an RNA-binding protein, zipcode binding protein 2 (ZBP2) was required for this localization to occur. (42) It is possible that this clustering of the mRNA in one region of the cell enhances mRNA stability or translational efficiency so that more protein can be produced. In the case of AR, this mechanism would allow for high protein accumulation that could push the prostate cancer cells to continue to grow and divide in lower levels of androgen.

In our discussion of this RNA localization pattern, it is also important to bring up that localized RNA granules in mammalian cells are thought to be stress granules, which are translationally inactive stores that when locally released can suddenly become translationally active to produce a localized rapid burst of protein when the cell is under stress. Perhaps these AR mRNA granules are actually stress granules of stabilized

60

mRNA that will become translationally active when needed in order to produce a sudden large supply of AR protein. Co-staining LNCaP and C4-2 cells for translational machinery proteins such as eukaryotic translation initiation factor 4G (eIF4G) and determining whether or not these proteins colocalize with the AR mRNA granules would indicate whether or not these are translationally inactive stress granules. (47)

The method of AR mRNA detection was optimized through the use of the two beacons in tandem and by changing the backbone chemistry of the beacons to a chimeric formulation with 2'-*O*-Me RNA bases in the hybridization domain. This optimized dual chimeric beacon approach allowed for enhancement of the signal-to-background ratio in live cell imaging. The enhanced signal permitted for a decrease in imaging exposure time, which allowed for a more dramatic difference in AR mRNA signal between AR+ LNCaP cells and AR- DU-145 cells.

The dual chimeric beacon system was validated through a series of tests in order to ensure that AR mRNA was being targeted specifically. Visualizing total RNA in LNCaP cells was a strong piece of evidence in this case. The RNA localization pattern in LNCaP cells is granular in nature, matching the structures seen by our beacons. The fact that several mRNAs, including rat AR mRNA, have been shown to localize in granules (41,44) coupled with the fact that RNA-binding proteins known to associate with AR mRNA have also been shown to localize in granules (43) further encourages our results. The ability of the beacons to distinguish between AR+ LNCaP cells and AR- DU-145 cells was another strong piece of evidence supporting the specificity of these probes.

61

Many methods for modulating the level of AR mRNA were attempted to add support to the validation of our molecular beacon system. siRNA, Vitamin D treatment, and hormone starvation treatment proved to be poor methods for validating our beacons either due to the effect of the treatment on cell morphology or the failure of the method to cause a significant change in AR mRNA expression that would be visually detectable.

The effects that certain siRNA transfection reagents had on cell morphology were disturbing. While most biologists care simply that they are able to knockdown their targeted protein with siRNA, they do not often consider the effects of the reagents themselves on cell morphology and function. The fact that Lipofectamine™ 2000 induced the formation of large vesicles that often became "beacon traps", unfortunately prevented us from using this method as a means for validating our probe system, but more importantly it raised the question of what are these transfection reagents really doing to our cells. If such a drastic change in morphology is occurring with reagent application, is it fair to say that a non-treated cell is functionally similar to a reagent-treated cell? Is the only difference between the two cells the level of the siRNA-targeted mRNA and protein, or are there more regulatory changes that are induced by the reagent? These questions remain unanswered and are outside the scope of this thesis, but they bring up an important point to be considered by molecular biologists using this technique. As for using siRNA as a method for beacon validation, without the answers to those questions, it would be very difficult to definitively use the results of this method as proof of beacon specificity, even if they did show the desired result.

Regulation of AR mRNA by thapsigargin, however, proved to be an effective and repeatable method for altering AR mRNA levels significantly. The ability of our beacon system to visually track the temporal change in AR mRNA expression due to

thapsigargin treatment and post-treatment recovery remains a key piece of evidence supporting the specificity of our system.

However, the fluorescence quantification of this treatment regimen did not produce as convincing results as the visualization itself. Fluorescence quantification was performed on deconvolved Z-stacks of 0.2 μm thick slices of cultured cells using the softWoRx image analysis package. Despite the obvious visual differences between time points in the thapsigargin treatment and recovery time course, when quantifying the fluorescence levels of the cells using this quantification method, minimal differences were observed. A reason for this could be that the contribution of the beacon fluorescence to the overall fluorescence in the cell is minimal due to a high level of background fluorescence picked up by the quantification system. When the average fluorescence per 1 $μm^3$ volume was calculated for areas on the glass slide without cells on it and this value was compared to the average fluorescence per 1 $μm^3$ cellular volume of non-treated LNCaP cells, it was found that the glass slide had an average of 78.91% of the fluorescence signal seen in non-treated cells. This means that a staggering amount of the fluorescence picked up could be due to non-beacon signal. The method for quantifying intracellular fluorescence levels needs to be examined further in order to remove noise that could be overshadowing actual differences in beacon fluorescence between cellular treatment groups. This raises questions concerning the best way to normalize the quantified cellular fluorescence by subtracting out background. Would it be appropriate to use the blank glass slide fluorescence for normalization, or would a cell without beacons in it be more appropriate, or would a dark area within a cell be the right choice? Using the glass slide seems the most straightforward, but does cell adherence to the slide change the amount of fluorescence emitted from the slide itself? Cells without beacons might have a different level and distribution of autofluorescence than cells containing beacons.

63

Selecting a dark area within a cell would be subjective and it would be difficult to ensure consistency from experiment to experiment and user to user.   Further exploration of this topic needs to occur in order to improve this method of fluorescence quantification enough to make it a viable tool in helping to prove probe specificity.

Once the AR mRNA dual chimeric beacon system had undergone several validation tests, we then determined that this system could be utilized to study posttranscriptional regulation of AR mRNA in prostate cancer cells. We were able to detect changes in AR mRNA state when LNCaP cells were stimulated with the synthetic androgen, R1881. After 24 hours of hormone stimulation, AR mRNA accumulated in large granules.   It is not known at the present time whether there is functional relevance to this AR mRNA accumulation. Since hormone stimulation of LNCaP cells is known to lead to increased production of AR protein, which in turn pushes the cells to continue to grow and divide, we speculate that this reorganization of AR mRNA into large clustered granules is to add to message stability and/or translational efficiency of the message, both of which would lead to increased protein production. It is uncertain at this time whether or not you could prove the reorganization of the AR mRNA in response to hormone stimulation contributes to this mechanism.

It would be interesting to take this hormone stimulation experiment one step further and see how the structure and localization of AR mRNA changes at time points between 0 and 24 hours. Once seeing how AR mRNA is regulated in LNCaP cells during this dramatic period of hormone stimulation, it would be interesting to switch to the androgen-independent C4-2 model cell line and see how it's regulation of AR mRNA differs during hormone stimulation. Since C4-2 cells are in the androgen-independent phase, would they respond to the hormone at all or would the changes be considerably

64

less dramatic? The answer to this is unsure, but if there is a differential response, perhaps the alteration in response could be used as a prognostic indicator for determining whether AR+ prostate cancer cells are in the androgen-dependent or androgen-independent state. It would first be necessary to determine if these localization patterns and changes are characteristic of other AR+ prostate cancer cells, not just LNCaP and C4-2 model cell lines. You could potentially determine whether this AR mRNA localization pattern and distribution change occurs in other cases of AR+ prostate cancer by visualizing the AR mRNA localization in AR+ prostate cancer cells that have already been characterized as androgen-dependent or androgen-independent and determining if they follow the trend of these model cell lines.

The AR mRNA detection system was also useful in showing differences in AR mRNA localization between the androgen-dependent LNCaP cells and their androgen-independent counterpart cell line, C4-2.   β-actin mRNA spatial localization seen in fibroblasts and neurons (41,42) has been shown to serve the purpose of providing a localized concentration of β-actin protein in these cells. (48,49) If these AR mRNA granules are truly stress granules, perhaps the alteration in localization between LNCaP and C4-2 cells is due to the need for rapid large bursts of AR protein more homogenously in C4-2 cells in order to enable these cells to survive in low androgen levels. By having a more dispersed production of AR, the likelihood of AR encountering DHT in these cells should increase, helping push the AR growth pathway.

It has not been shown at this time whether or not these changes in AR mRNA structure and localization occur in other AR+ prostate cancer cells, besides LNCaP cells, as they transition from androgen-dependent to androgen-independent. If this was shown to be a common phenomenon, determining AR mRNA localization could prove to be a useful

65

prognostic indicator of when prostate cancer is in the androgen-dependent or androgen-independent phase. Again, it would be necessary to look at AR mRNA localization and distribution changes in other AR+ prostate cancer cells to see if this trend is not just a phenomenon of the LNCaP and C4-2 cell lines.

Future experiments can also be conducted to show how this change in AR mRNA organization occurs over the course of the transition between androgen-dependence to androgen-independence. LNCaP cells can be transformed into androgen-independent C4-2 cells by repeated hormone starvation over a period of several months (50) or some researchers have shown it can be done through the upregulation of certain factors, such as Protein Kinase Cε, in a much shorter time frame, on the order of a week. (51) Visualizing changes in AR mRNA localization over this important transition could allow one to not only make the black-or-white call between an androgen-dependent or androgen-independent diagnosis, but allow for the determination of whether the cancer cells are in the process of making that critical transition.

Our collaborators at Emory University, as well as others, are interested in the role that prostate tumor stroma plays is the progression and regulation of prostate cancer cells. (52) It has already been shown that the co-culture of tumor and stromal cells can have a profound impact on the population of stromal cell mRNA interacting with a specific RNA-binding protein. Dr. Jack Keene's group co-cultured PY4.1 endothelial cells with 4T1 breast cancer cells and found that the subpopulation of mRNA interacting with poly(A) binding protein (PABP) in the co-cultured stromal cells differed from those in the stromal cells cultured independently. PABP-interacting mRNAs that were upregulated in response to the tumor cells included Cyclins, proliferation factors, and transcription factors. (53) Since cancer cells can have a profound impact on mRNA regulation in

66

stromal cells, it is logical that the inverse would be true as well. It would be of interest to

co-culture both LNCaP and C4-2 prostate cancer cell lines with stromal cells to see if the

posttranscriptional regulation of AR mRNA changes. Repeating the hormone stimulation

experiments in the presence of stromal cells and seeing how the prostate cancer cells

respond in their regulation of AR mRNA could provide insight into the importance of

stromal cell interactions in these regulatory mechanisms.

REFERENCES

1.   Feldman, B.J. and Feldman, D. (2001) The development of androgen-independent prostate cancer. *Nature Reviews Cancer*, **1**, 34.

2.   Setlur, S.R. and Rubin, M.A. (2005) Current Thoughts on the Role of the Androgen Receptor and Prostate Cancer Progression. *Advances in Anatomic Pathology*, **12**, 265-270.

3.   Gelmann, E.P. (2002) Molecular Biology of the Androgen Receptor. *J Clin Oncol*, **20**, 3001-3015.

4.   Meyer, H.-A., Ahrens-Fath, I., Sommer, A. and Haendler, B. (2004) Novel molecular aspects of prostate carcinogenesis. *Biomedicine & Pharmacotherapy*, **58**, 10-16.

5.   Shand, R.L. and Gelmann, E.P. (2006) Molecular biology of prostate-cancer pathogenesis. *Current Opinion in Urology*, **16**, 123-131.

6.   Peehl, D.M. (2001) Basic Science of Hormonal Therapy for Prostate Cancer. *Reviews in Urology*, **3**, S15-S22.

7.   Yeap, B.B., Wilce, J.A. and Leedman, P.J. (2004) The androgen receptor mRNA. *BioEssays*, **26**, 672-682.

8.   Hollams, E.M., Giles, K.M., Thomson, A.M. and Leedman, P.J. (2002) mRNA Stability and the Control of Gene Expression: Implications for Human Disease. *Neurochemical Research*, **27**, 957-980.

9.   Eberhardt, W., Doller, A., Akool, E.-S. and Pfeilschifter, J. (2007) Modulation of mRNA stability as a novel therapeutic approach. *Pharmacology & Therapeutics*, **114**, 56-73.

10.   DeJong, E.S., Luy, B. and Marino, J.P. (2002) RNA and RNA-Protein Complexes as Targets for Therapeutic Intervention. *Current Topics in Medicinal Chemistry*, **2**, 289.

11.   Rhee, W.J., Santangelo, P.J., Jo, H. and Bao, G. (2008) Target accessibility and signal specificity in live-cell detection of BMP-4 mRNA using molecular beacons. *Nucleic Acids Research*, **36**, e30.

12.   Santangelo, P.J., Nitin, N. and Bao, G. (2006) Nanostructured probes for RNA detection in living cells. *Annals of Biomedical Engineering*, **34**, 39-50.

13.   Santangelo, P.J., Nitin, N. and Bao, G. (2005) Direct visualization of mRNA colocalization with mitochondria in living cells using molecular beacons. *Journal of Biomedical Optics*, **10**, 44025.

14.   Yeap, B.B. and al, e. (2002) Novel Binding of HuR and Poly(C)-binding Protein to a Conserved UC-Rich Motif within the 3'-Untranslated Region of the Androgen Receptor Messenger RNA. *The Journal of Biological Chemistry*, **277**, 27183-27192.

15. Wilce, J.A., Leedman, P.J. and Wilce, M.C.J. (2002) RNA-Binding Proteins That Target the Androgen Receptor mRNA. *IUBMB Life*, **54**, 345-349.

16. Quarmby, V.E., Yarbrough, W.G., Lubahn, D.B., French, F.S. and Wilson, E.M. (1990) Autologous down-regulation of androgen receptor messenger ribonucleic acid. *Molecular Endocrinology*, **4**, 22-28.

17. Yeap, B.B., Krueger, R.G. and Leedman, P.J. (1999) Differential Posttranscriptional Regulation of Androgen Receptor Gene Expression by Androgen in Prostate and Breast Cancer Cells. *Endocrinology*, **140**, 3282-3291.

18. Arnold, J.T., Le, H., McFann, K.K. and Blackman, M.R. (2005) Comparative effects of DHEA vs. testosterone, dihydrotestosterone, and estradiol on proliferation and gene expression in human LNCaP prostate cancer cells. *Am J Physiol Endocrinol Metab*, **288**, E573-584.

19. Wolf, D.A., Herzinger, T., Hermeking, H., Blaschke, D. and Horz, W. (1993) Transcriptional and Posttranscriptional Regulation of Human Androgen Receptor Expression by Androgen. *Molecular Endocrinology*, **7**, 924-936.

20. Krongrad, A., Wilson, C.M., Wilson, J.D., Allman, D.R. and McPhaul, M.J. (1991) Androgen increases androgen receptor protein while decreasing receptor mRNA in LNCaP cells. *Molecular and Cellular Endocrinology*, **76**, 79-88.

21. Tyagi, S. and Kramer, F.R. (1996) Molecular beacons: probes that fluoresce upon hybridization. *Nature Biotechnology*, **14**, 303-308.

22. Santangelo, P.J., Nix, B., Tsourkas, A. and Bao, G. (2004) Dual FRET molecular beacons for mRNA detection in living cells. *Nucleic Acids Research*, **32**, e57.

23. Tsourkas, A., Behlke, M.A. and Bao, G. (2002) Hybridization of 2'-O-methyl and 2'-deoxy molecular beacons to RNA and DNA targets. *Nucleic Acids Research*, **30**, 5168-5175.

24. Nitin, N., Santangelo, P.J., Kim, G., Nie, S. and Bao, G. (2004) Peptide-linked molecular beacons for efficient delivery and rapid mRNA detection in living cells. *Nucleic Acids Research*, **32**, e58.

25. Santangelo, P.J., Nitin, N., LaConte, L., Woolums, A. and Bao, G. (2006) Live-Cell Characterization and Analysis of a Clinical Isolate of Bovine Respiratory Syncytial Virus, Using Molecular Beacons. *Journal of Virology*, **80**, 682-688.

26. Santangelo, P.J. and Bao, G. (2007) Dynamics of filamentous viral RNPs prior to egress. *Nucleic Acids Research*, **35**, 3602-3611.

27. Medley, C.D., Drake, T.J., Tomasini, J.M., Rogers, R.J. and Tan, W. (2005) Simultaneous Monitoring of the Expression of Multiple Genes Inside of Single Breast Carcinoma Cells. *Anal. Chem.*, **77**, 4713-4718.

28. Tyagi, S. and Alsmadi, O. (2004) Imaging native beta-actin mRNA in motile fibroblasts. *Biophysical Journal*, **87**, 4153-4162.

29. Zuker, M. (2003) Mfold web server for nucleic acid folding and hybridization prediction. *Nucl. Acids Res.*, **31**, 3406-3415.

30. Bieche, I., Parfait, B., Tozlu, S., Lidereau, R. and Vidaud, M. (2001) Quantitation of androgen receptor gene expression in sporadic breast tumors by real-time RT-PCR: evidence that MYC is an AR-regulated gene. *Carcinogenesis*, **22**, 1521-1526.

31. Yacoub, A., Park, J.S., Qiao, L., Dent, P. and Hagan, M.P. (2001) MAPK dependence of DNA damage repair: ionizing radiation and the induction of expression of the DNA repair genes XRCC1 and ERCC1 in DU145 human prostate carcinoma cells in a MEK1/2 dependent fashion. *International Journal of Radiation Biology*, **77**, 1067 - 1078.

32. Rondinelli, R.H., Epner, D.E. and Tricoli, J.V. (1997) Increased glyceraldehyde-3-phosphate dehydrogenase gene expression in late pathological stage human prostate cancer. *Prostate Cancer & Prostatic Diseases*, **1**, 66.

33. Wright, M.E., Tsai, M.-J. and Aebersold, R. (2003) Androgen Receptor Represses the Neuroendocrine Transdifferentiation Process in Prostate Cancer Cells. *Mol Endocrinol*, **17**, 1726-1737.

34. Ray, M.R., Wafa, L.A., Cheng, H., Snoek, R., Fazli, L., Gleave, M. and Rennie, P.S. (2006) Cyclin G-associated kinase: A novel androgen receptor-interacting transcriptional coactivator that is overexpressed in hormone refractory prostate cancer. *International Journal of Cancer*, **118**, 1108-1119.

35. Zhao, X.-Y., Ly, L.H., Peehl, D.M. and Feldman, D. (1999) Induction of Androgen Receptor by 1{alpha},25-Dihydroxyvitamin D3 and 9-cis Retinoic Acid in LNCaP Human Prostate Cancer Cells. *Endocrinology*, **140**, 1205-1212.

36. Gong, Y., Blok, L.J., Perry, J.E., Lindzey, J.K. and Tindall, D.J. (1995) Calcium regulation of androgen receptor expression in the human prostate cancer cell line LNCaP. *Endocrinology*, **136**, 2172-2178.

37. Lin, X.S., Denmeade, S.R., Cisek, L. and Isaacs, J.T. (1997) Mechanism and role of growth arrest in programmed (apoptotic) death of prostatic cancer cells induced by thapsigargin. *The Prostate*, **33**, 201-207.

38. Skryma, R., Mariot, P., Bourhis, X., Coppenolle, F., Shuba, Y., Abeele, F.V., Legrand, G., Humez, S., Boilly, B. and Prevarskaya, N. (2000) Store depletion and store-operated Ca2+ current in human prostate cancer LNCaP cells: involvement in apoptosis. *The Journal of Physiology*, **527**, 71-83.

39. Balañá, M.E., Alvarez Roger, C., Dogour, A.V. and Kerner, N.A. (2004) Antiandrogen oligonucleuotides: active principles in hair- and skin-derived culture cells. *Journal of Drugs In Dermatology*, **3**, 287-294.

40. Hamy, F., Brondani, V., Spoerri, R., Rigo, S., Stamm, C. and Klimkait, T. (2003) Specific block of androgen receptor activity by antisense oligonucleotides. *Prostate Cancer & Prostatic Diseases*, **6**, 27.

70

41.   Bassell, G.J., Oleynikov, Y. and Singer, R.H. (1999) The travels of mRNAs through all cells large and small. *FASEB J.*, **13**, 447-454.

42.   Gu, W., Pan, F., Zhang, H., Bassell, G.J. and Singer, R.H. (2002) A predominantly nuclear protein affecting cytoplasmic localization of {beta}-actin mRNA in fibroblasts and neurons. *J. Cell Biol.*, **156**, 41-52.

43.   Antic, D. and Keene, J.D. (1998) Messenger ribonucleoprotein complexes containing human ELAV proteins: interactions with cytoskeleton and translational apparatus. *J Cell Sci*, **111**, 183-197.

44.   Prins, G.S. and Woodham, C. (1995) Autologous regulation of androgen receptor messenger ribonucleic acid in the separate lobes of the rat prostate gland. *Biol Reprod*, **53**, 609-619.

45.   Tuohimaa, P., Lyakhovich, A., Aksenov, N., Pennanen, P., Syvälä, H., Lou, Y.R., Ahonen, M., Hasan, T., Pasanen, P., Bläuer, M. *et al.* (2001) Vitamin D and prostate cancer. *The Journal of Steroid Biochemistry and Molecular Biology*, **76**, 125-134.

46.   Wu, H.-C., Hsieh, J.-T., Gleave, M.E., Brown, N.M., Pathak, S. and Chung, L.W.K. (1994) Derivation of androgen-independent human LNCaP prostatic cancer cell sublines: Role of bone stromal cells. *International Journal of Cancer*, **57**, 406-412.

47.   Krichevsky, A.M. and Kosik, K.S. (2001) Neuronal RNA Granules: A Link between RNA Localization and Stimulation-Dependent Translation. *Neuron*, **32**, 683-696.

48.   Etkin, L.D. and Lipshitz, H.D. (1999) RNA localization. *FASEB J.*, **13**, 419-420.

49.   St. Johnston, D. (2005) Developmental Cell Biology: Moving messages: the intracellular localization of mRNAs. *Nature Reviews Molecular Cell Biology*, **6**, 363-375.

50.   Gao, M., Ossowski, L. and Ferrari, A.C. (1999) Activation of Rb and decline in androgen receptor protein precede retinoic acid-induced apoptosis in androgen-dependent LNCaP cells and their androgen-independent derivative. *Journal of Cellular Physiology*, **179**, 336-346.

51.   Wu, D., Foreman, T.L., Gregory, C.W., McJilton, M.A., Wescott, G.G., Ford, O.H., Alvey, R.F., Mohler, J.L. and Terrian, D.M. (2002) Protein Kinase Cε Has the Potential to Advance the Recurrence of Human Prostate Cancer. *Cancer Res*, **62**, 2423-2429.

52.   Cunha, G.R., Ricke, W., Thomson, A., Marker, P.C., Risbridger, G., Hayward, S.W., Wang, Y.Z., Donjacour, A.A. and Kurita, T. (2004) Hormonal, cellular, and molecular regulation of normal and neoplastic prostatic development. *The Journal of Steroid Biochemistry and Molecular Biology*, **92**, 221-236.

53.   Penalva, L., Burdick, M., Lin, S., Sutterluety, H. and Keene, J. (2004) RNA-binding proteins to assess gene expression states of co-cultivated cells in response to tumor cells. *Molecular Cancer*, **3**, 24.

71